On Non-Binary Constellations for Channel-Encoded Physical Layer Network Coding

by

Zahra Faraji-Dana

A thesis
presented to the University of Waterloo
in fulfillment of the
thesis requirement for the degree of
Master of Applied Science
in
Electrical and Computer Engineering

Waterloo, Ontario, Canada, 2012

I hereby declare that I am the sole author of this thesis. This is a true copy of the thesis, including any required final revisions, as accepted by my examiners.

I understand that my thesis may be made electronically available to the public.

Abstract

This thesis investigates channel-coded physical layer network coding, in which the relay directly transforms the noisy superimposed channel-coded packets received from the two end nodes, to the network-coded combination of the source packets. This is in contrast to the traditional multiple-access problem, in which the goal is to obtain each message explicitly at the relay. Here, the end nodes A and B choose their symbols, S_A and S_B, from a small non-binary field, $\mathbb{F}$, and use non-binary PSK constellation mapper during the transmission phase. The relay then directly decodes the network-coded combination $aS_A + bS_B$ over $\mathbb{F}$ from the noisy superimposed channel-coded packets received from two end nodes. Trying to obtain S_A and S_B explicitly at the relay is overly ambitious when the relay only needs $aS_B + bS_B$. For the binary case, the only possible network-coded combination, $S_A + S_B$ over the binary field, does not offer the best performance in several channel conditions. The advantage of working over non-binary fields is that it offers the opportunity to decode according to multiple decoding coefficients (a, b). As only one of the network-coded combinations needs to be successfully decoded, a key advantage is then a reduction in error probability by attempting to decode against all choices of decoding coefficients. In this thesis, we compare different constellation mappers and prove that not all of them have distinct performance in terms of frame error rate. Moreover, we derive a lower bound on the frame error rate performance of decoding the network-coded combinations at the relay. Simulation results show that if we adopt concatenated Reed-Solomon and convolutional coding or low density parity check codes at the two end nodes, our non-binary constellations can outperform the binary case significantly in the sense of minimizing the frame error rate and, in particular, the ternary constellation has the best frame error rate performance among all considered cases.

Acknowledgements

First and foremost, I would like to express my deep gratitude to my supervisor, Professor Patrick Mitran, for his support and encouragement and for giving me the opportunity to do this work.

Dedication

This is dedicated to the one I love.

Contents

List of Tables

List of Figures

Chapter 1

Introduction

1.1 History

In the past few decades, the demand for network capacity has substantially increased in order to support high data rate services such as high speed internet and multimedia applications. Today, communication networks need to meet such growing demands with high spectral efficiency, low energy consumption and high mobility [1].

In a network consisting of source nodes, destination nodes and intermediate nodes, each source node wants to transmit its own packet to a set of destination nodes with the assistance of the intermediate nodes. Given the limitations in bandwidth and energy, what is the best network performance and how it can be achieved are basic questions in wireless network design. In traditional communications, the information to be sent from a source node to a destination node is conveyed through a series of intermediate nodes by the store-and-forward switching, a method in which intermediate nodes forward the received data to the next node without modifying its content.

Network coding has recently emerged as a new paradigm for communication in networks that require a significantly higher network capacity [2–4]. Due to its wide range of foreseen applications, network coding has received much attention from many research groups in a variety of fields: information theory, networking, etc. The main idea of network coding is to use the intermediate nodes for mixing and processing information from multiple links. In this way, fewer time intervals are needed to convey a specific amount of information through the network, and hence the network throughput can be increased. The well-known butterfly network demonstrates the capabilities of the net-

work coding technique in increasing the network throughput. In the butterfly network shown in Fig. 1.1, source node S has two bits of data, a and b, to send to destinations D and R. We assume that all links in the network are error free and have unit capacity. When network coding is used (see Fig. 1.1(a)) the intermediate node X mixes the incoming data a and b to achieve the exclusive-or (XOR) of the two, i.e., $a \oplus b$. Knowing both a and $a \oplus b$, D can obtain the data bit b by taking the XOR of a and $a \oplus b$. Similarly, R obtains the data bit a. For the same butterfly example, when the store-and-forward technique is used, see Fig. 1.1(b), each intermediate node forwards what it has received to its neighbor nodes. Since the capacity of the link between X and Y is one, the node X can only transmit one bit at a time and hence, the traditional store-and-forward technique requires one time slot more than the network coding.

(a) network coding   (b) store-and-forward
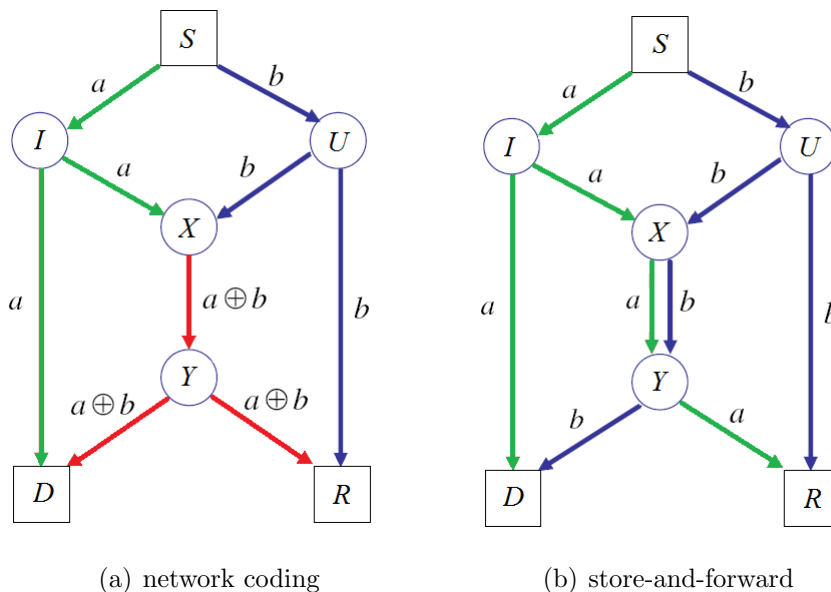
Figure 1.1: The butterfly network

Network coding was first introduced for wired networks. However, there have recently been some efforts to apply network coding to wireless networks [5–8]. In [5], the authors establish a new framework for network coding in ad hoc wireless networks. They consider a simple wireless network topology to illustrate how network coding can improve throughput and energy efficiency beyond routing solutions. They further extend the network coding problem to general wireless networks in conjunction with scheduling-based medium access control. They present numerical results to compare throughput and energy efficiency of network coding and routing solutions. In [6], some of the the main features of network coding that are most relevant to wireless networks have been

investigated, in particular, the fact that random distributed network coding is asymptotically optimal for wireless networks with and without packet erasure is discussed. Reference [7] studies network coding capacity for random wireless networks with a more realistic model, where wireless networks are modeled by random geometric graphs with interference and noise, and thus, the capacities of links are not independent. Reference [7] shows that in single-source-multiple-destination and multiple-sources-multiple-destination scenarios, the network coding capacity for random wireless networks exhibits a concentration behavior around the mean value of the minimum cut under some mild conditions. In [8], a new architecture for wireless mesh networks called COPE is proposed, in which routers mix packets from different sources to increase the information content of each transmission and forward them. It is shown that intelligently mixing packets increases network throughput. The authors address the common case of uni-cast traffic, dynamic and potentially bursty flows, and practical issues facing the integration of network coding in the current network stack. They show that using COPE at the forwarding layer, without modifying routing and higher layers, increases network throughput.

In wireless networks, interference has been traditionally considered to be destructive, and simultaneous transmissions are usually avoided in order to prevent interference. On the other hand, interference is nothing but the sum of delayed and attenuated signals, and may in fact contain beneficial information. This point of view suggests the use of decoding techniques to process interference in wireless networks, instead of treating it as a nuisance to be avoided [9]. Inspired by the principle of network coding, physical-layer network coding (PNC) is a technique in which the intermediate node relays a functions of the decoded incoming packets, usually linear combinations, rather than the packets individually. In PNC, the linear combination(s) are inferred directly from the received signal at the intermediate node. The key idea of PNC has been proposed independently by several research groups in 2006: Zhang, Liew, and Lam [10], Popovski and Yomo [11], and Nazer and Gastpar [12]. The authors of [10] considered a very simple channel model for intermediate nodes, in which the received signal at the relay Y_R is given as $Y_R = X_A + X_B + Z_R$, where X_A and X_B are BPSK signals, Z_R is Gaussian noise, and, as in a simple network coding system, the relay attempts to decode the XOR of the transmitted messages. They have shown that this simple strategy significantly improves the throughput of a two-way relaying channel. However, in [11], a more general channel model that captures the effects of fading and probable phase misalignment is considered. Then, the received signal at the relay is $Y_R = H_A X_A + H_B X_B + Z_R$, where H_A and H_B are known complex-valued channel gains, and the relay again attempts to decode the XOR of the transmitted messages. The authors show that in a large range of signal-to-noise ratios (SNR), their strategy outperforms the conventional relaying strategies such as amplify-and-forward and decode-and-forward, in a two-way relaying system. Because

of its simplicity and the substantial benefits foreseen in it [13,14], PNC has gained much attention since 2006. Many strategies have been proposed for PNC, with a particular focus on two-way relaying, where end nodes A and B exchange information with the help of relay node R, shown in Fig. 1.2. We assume that each node is equipped with a unidirectional antenna and the channel is half duplex. Thus, transmission and reception at a particular node must happen in different time slots. We also assume that there is no direct link between nodes A and B. In [10] and [11], three different protocols for bidirectional relaying are presented. Compared to the 4- and 3-stage protocols, the 2-stage protocol can improve throughput because of its effective time usage.
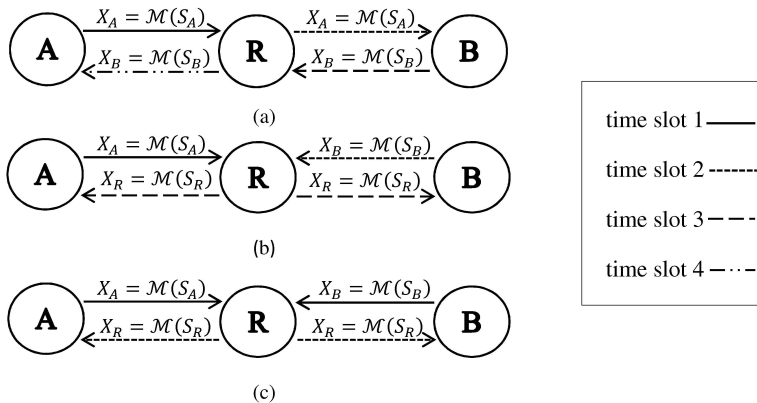
Figure 1.2: Two-way relaying protocols: (a) traditional transmission, (b) straightforward network coding scheme, (c) physical layer network coding.

In this thesis, we concentrate on the relaying scheme with PNC, shown in Fig. 1.2(c), which is a two-phase transmission scheme consisting of an uplink phase and a downlink phase. In the uplink phase, termed *multiple access (MAC)* stage, nodes A and B transmit packets to the relay node R simultaneously. Relay node R then constructs a network-coded packet based on the overlapped signals received from nodes A and B. In the downlink phase, called the *broadcast (BC)* stage, the relay R broadcasts the packet to nodes A and B. Knowing its own information *a priori*, node A (B) can decode the data from node B (A), using the broadcasted signal from relay R.

In [15], the authors investigate the conditions for maximization of the two-way rate for the following schemes: (1) the decode-and-forward (DF) 3-step schemes (2) three different schemes with two steps: amplify-and-forward, joint decode-and-forward (JDF) and denoise-and-forward (DNF). They show that, while the DNF scheme has a potential to offer the best two-way rate, for some SNR configurations of the source-relay links, JDF yields identical maximal two-way rate as the upper bound on the rate for DNF.

In [16], the authors investigate the usage of structured and lattice codes in a scenario for two-way relaying. The maximal achievable rate is calculated for the proposed joint physical-network layer code. In [17], Nazer et al. study the problem of recovering a function of data simultaneously transmitted from multiple sources through a common channel and find an achievable rate for this channel. In [18], Nazer et al propose a compute-and-forward strategy, where the relays decode linear functions of transmitted messages, knowing the channel coefficients. In their model, after decoding these linear combinations, the relays send them to the terminals, which given enough linear combinations, can solve for their desired messages. The authors use lattice codes whose algebraic structure ensures that integer combinations of codewords can be decoded reliably. In [19], Zhang et al. propose a PNC scheme to coordinate transmissions among nodes. They show that PNC can potentially achieve 100% and 50% throughput increase compared to traditional transmission and straightforward network coding, respectively, in multi-hop networks and the information-theoretic capacity of PNC is almost double that of traditional transmission in SNRs higher than 0dB.

In [20], a novel method called analog network coding is proposed, in which instead of forwarding packets, routers forward the interfering signals (not the mixed bits) and the destination leverages network-level information to cancel the interference and recover the intended signal. Such an approach doubles the capacity of the canonical two-way relay network.

The main requirement of PNC is synchronization among nodes, which has been addressed in [21]. The authors of [21] investigate the impact of imperfect synchronization on PNC and show that with BPSK modulation, PNC still yields significantly higher capacity than straightforward network coding in the presence of synchronization errors. Furthermore, they show that the network capacity achieved by PNC is superior to that achieved by the traditional methods even in the extreme case where synchronization is not performed at all. In [22], the authors considered the use of non-coherent detection at the relay for a PNC scenario. The proposed non-coherent relay does not require phase synchronism. Using a turbo code, the non-coherent physical-layer network coding system offers better throughput compared to the corresponding link-layer network coding system, when either channel statistics or fading amplitude information are provided to the relay.

Network coding at the relay node R is challenging because channel gains and noise at the MAC stage randomly perturb the received overlapped packets. The relay's observation during the MAC stage is the basis of the decision process to determine the information to be transmitted in the BC stage. In [23], the authors introduce a modulation design method for dealing with this randomness which improves the throughput significantly. Their scheme allows the use of unusual 5-ary modulation in the BC stage

while QPSK modulation is used in the MAC stage. In their model, a DNF scheme is implemented by the relay node.

In [24], the overlapped BPSK-modulated signals in the relay node R are transformed directly to the network-coded packet. The authors adopt a repeat accumulate (RA) channel code at the two end nodes and redesign the belief propagation decoding algorithm of the RA code to suit the PNC configuration. Their scheme is efficient in terms of bit error rate without adding complexity.

In [25], the authors introduce two new PNC categories: PNCF (PNC over finite field) and PNCI (PNC over infinite field) according to whether the network-code field adopted is finite of infinite. For each of PNCF and PNCI, they consider two specific estimation techniques for dealing with noise in the mapping process. They have assumed that the source packets are not channel-encoded and that QPSK modulation is adopted at the end terminal. However, the idea of adopting channel-coding schemes at the end nodes has been investigated in [26, 27]. In [26], the authors investigate an LDPC encoded two-way relaying system, in which a simple interference cancelation joint decoder is implemented at the relay. The bit error rate performance of their simple interference cancelation joint decoder is shown to be close to the existing sub-optimal belief propagation joint decoder. They show that, for their configuration, the required SNR at the source is much less than that of the single user channel with the same bit error rate.

In [28], the authors propose a distributed PNC scheme that obviates the need for synchronization and is robust to random packet loss and delay. The proposed system is simple to implement and incurs less overhead than the practical network coding system.

In early 2011, Lu, L., *et al.* [29] present the first implementation of a two-way relay network based on the principle of PNC. Two comprehensive surveys about PNC can be found in [30, 31].

1.2   Thesis Contributions

In this thesis, the end nodes A and B choose their symbols, S_A and S_B, from a small finite field $\mathbb{F} = GF(q)$. The symbols are then q-PSK modulated and sent to the relay. We propose a PNCF scheme [25] for directly decoding a network-coded combination, i.e., $aS_A + bS_B$ over $\mathbb{F}$, from the overlapped channel-coded signals received from the two end nodes (plus noise), $Y_R = H_A X_A + H_B X_B + Z_R$. This can be seen as a compute-and-forward type strategy since a linear function of the transmitted messages is inferred from the noisy linear combination provided by the channels. However, as opposed to lattice codes, the linear coding schemes here are a practical concatenation of Reed-Solomon and convolutional codes (RS-CC) and low-density parity check codes (LDPC)

over small non-binary fields, which are suitable for both quasi-static and fast fading channels. To the best of our knowledge, practical physical-layer network coding for fast fading channels has not been addressed in the literature. We consider both quasi-static fading and fast fading channels in this thesis. Fast fading channels are a good model for frequency selective channels where orthogonal frequency division multiplexing (OFDM) is applied with subcarrier interleaving. Furthermore, due to the cyclic prefix of OFDM, if the two transmissions from the end nodes are not perfectly received in time at the relay, the timing error can be absorbed as part of the channel responses.

For the binary case, the only possible network-coded combination, $S_A + S_B$ over the binary field, does not offer the best performance in several channel conditions. In contrast, the unconventional non-binary constellations offer flexibility in choice of decoding coefficients (a, b). Therefore, the relay is capable of attempting to decode multiple network-coded combinations. If at least one of these network-coded combinations is decoded successfully, a correct decision will be made at the relay. Therefore, attempting to decode against all combinations (a, b) can decrease the probability of error at the relay. Later, we will see more on the advantages of attempting to decode different linear combinations.

We aim to compare cases when the end nodes use constellations of size 3, 4, and 5 with the conventional binary case. Simulation results suggest that further increasing the constellation size is not beneficial since, for a fixed transmission power, constellation points get closer to each other and the probability of error increases. For this very reason, without coding, the binary case has better performance. However, un-encoded transmission is not practical. When the end nodes employ channel coding, we find that non-binary constellations can outperform the binary case as decoding against all coefficients (a, b) provides greater benefit than the reduction in minimum distance costs.

Using q-PSK modulation, there are $q!$ different constellation mappers for arranging the constellation points on the circle. In this thesis, we investigate these mappers for fields $GF(3)$, $GF(2^2)$, and $GF(5)$. Exploiting the symmetric properties of the problem and using group theory arguments, we prove that the performance of different mappers in $GF(3)$ is the same in terms of frame error rate (FER) for *any* code (linear or nonlinear) employed at the end nodes. However, in $GF(2^2)$ the performance of different mappers is the same only if a linear code is adopted at the end nodes. For the field $GF(5)$, if the code is linear, we show that there are 4 different classes of constellation mappers with possibly different performance, which greatly reduce the search for the best mapping from $5! = 120$ cases to 4.

Moreover, employing Fano's inequality, we derive a lower bound on the FER performance of decoding the network-coded combinations at the relay in a PNC scenario.

All in all, the major contributions of this thesis are summarized as follow:

7

- We utilize non-binary constellations and directly decode network-coded combinations, $aS_A + bS_B$, over finite fields from the superimposed channel-coded packets, using either a practical concatenation of Reed-Solomon and convolutional codes, or an LDPC code.

- Working over non-binary finite fields offers multiple choices for decoding coefficients, a and b. We benefit from attempting to decode multiple network-coded combinations at the relay.

- We show that for a finite field $\mathbb{F}$, there are effectively only $|\mathbb{F}| - 1$ pairs of decoding coefficients that should be attempted by the decoder. There is no performance gain in attempting more.

- We investigate the performance of different $q-$PSK constellation mappers in terms of FER for $q \leq 5$. We prove that the number of constellation mappers with different performance is much less than the total constellation mappers, i.e., $q!$. Therefore, we do not need to consider all different constellation mappers in the search for the best one.

- We find a lower bound using Fano's inequality on the FER performance of decoding the network-coded combinations at the relay.

- When using RS-CC codes, for quasi-static fading channels, finite fields $GF(3)$, $GF(2^2)$ and $GF(5)$ outperform the binary case. For fast fading channels, finite fields $GF(3)$ and $GF(2^2)$ outperform the binary case only by taking advantage of attempting to decode multiple network-coded combinations.

- When using LDPC codes, for quasi-static fading and fast fading channel, the finite fields $GF(3)$ and $GF(2^2)$ outperform the binary case only by taking advantage of attempting to decode multiple network-coded combinations.

- $GF(3)$ has the best performance among all other fields, when RS-CC or LDPC channel coding is adopted at the MAC stage.

1.3   Outline of Thesis

The rest of this thesis is organized as follows: In Chapter 2, we introduce the basic system model, go through the details of the network coding at the relay and explain the physical layer network coding over non-binary fields. In Chapter 3, we obtain an analytic expression for the error probability performance of the un-encoded PNC,

using the minimum distance analysis. We use this expression to compare the bit error rate (BER) performance of the un-encoded PNC over non-binary fields with that of the binary field. In Chapter 4, we introduce the channel coding schemes employed at the end nodes and illustrate the problem formulation if a channel coding scheme is used. In Chapter 5, we investigate the performance of different constellation mappers in terms of FER, using the symmetric properties of the problem and group theory arguments. In Chapter 6, employing Fano's inequality, we derive a lower bound on the FER performance of directly decoding the network-coded combinations at the relay. In Chapter 7, simulation results are presented. Finally, conclusions and discussions on future research are given in Chapter 8.

Chapter 2

Bidirectional Relaying

2.1 Multiple Access (MAC) Stage

We denote by $S_A, S_B \in \mathbb{F}$ the source data from A and B, respectively. We let $\mathcal{M} : \mathbb{F} \to \mathbb{C}$ denote a $q-$PSK constellation mapper used at the MAC stage. The signals transmitted from sources A and B are $X_A = \mathcal{M}(S_A)$ and $X_B = \mathcal{M}(S_B)$. We assume that the constellation points have unit energy. The received signal at the relay node R is expressed as

$$Y_R = H_A X_A + H_B X_B + Z_R, \tag{2.1}$$

where H_A and H_B are complex-valued channel gains from the end nodes A and B to the relay node R, respectively. We assume that Z_R is complex-valued additive white Gaussian noise (AWGN) with variance $\sigma^2 = N_0$. For given constellation mapper $\mathcal{M}$ and channel gains H_A and H_B, we will call the following set the *received constellation*:

$$\mathbf{M}_{\mathcal{M}}(H_A, H_B) = \{H_A \mathcal{M}(S_A) + H_B \mathcal{M}(S_B) | S_A, S_B \in \mathbb{F}\}.$$

For simplicity of analysis and exposition, we assume a time-synchronous communication system. Again, this is a reasonable assumption, as an OFDM-based bidirectional relaying system is robust to time synchronization errors due to the cyclic prefix.

2.2 Network Coding at the Relay

In network coding the critical issue is how the relay R makes use of Y_R to construct a packet to broadcast to the end nodes A and B in the downlink phase such that destinations are able to extract the information addressed to them from the relayed signal. As long as the relay node R can transmit the necessary information to the end nodes for extraction of the intended information, the end-to-end communication will be successful. The relay node R is not the intended destination of the data from the source and hence it does not need the individual information transmitted by nodes A and B. By leveraging on this observation, we can increase the space of available relaying strategies. In this section we discuss several techniques, in which the relay node does not decode the source data individually. The strategies without decoding (the individual source data) at the relay are not novelty applied to the two-way relaying, and they have already been used in one-way relaying. Nevertheless, there are novel strategies such as denoise-and-forward (DNF) that are brought by the distinctive features of the two-way relaying scenario. In this section, we explain four two-step strategies.

2.2.1 Amplify-and-Forward (AF)

In amplify-and-forward (AF) strategy, the relay R amplifies and broadcasts the noisy superimposed received packet Y_R from the uplink phase, such that the signal transmitted in the broadcast phase is

$$S_R = \alpha Y_R = \alpha H_A X_A + \alpha H_B X_B + \alpha Z_R \tag{2.2}$$

where α is the amplification factor and is chosen as

$$\alpha = \sqrt{\frac{1}{|H_A|^2 + |H_B|^2 + N_0}} \, , \tag{2.3}$$

to make the average per-symbol transmitted energy at the relay R equal to one. The symbol received by A is the amplified version of the symbol received by R in the MAC stage plus noise

$$
\begin{aligned}
Y_A &= \alpha H_A Y_R + Z_A \\
&= \alpha H_A{}^2 X_A + \alpha H_A H_B X_B + \alpha H_A Z_R + Z_A
\end{aligned} \tag{2.4}
$$

where (2.4) is obtained under fixed channel gain assumption. Assuming that A knows X_A, H_A, H_B, and α, then it can remove the contribution of $\alpha H_A^2 X_A$ from Y_A and obtain

$$R_A = \alpha H_A H_B X_B + \alpha H_A Z_R + Z_R, \tag{2.5}$$

which is a Gaussian channel for receiving X_B with SNR:

$$SNR = \frac{\alpha^2 |H_A|^2 |H_B|^2}{(\alpha^2 |H_A|^2 + 1) N_0}. \tag{2.6}$$

Knowing the SNR, node A is able to estimate S_B.

2.2.2   Denoise-and-Forward (DNF)

Although the relay does not decode the messages from A and B, it can process the received signal Y_R. These strategies are called denoise-and-forward (DNF) in order to emphasize that the noise is mitigated, but the source data are not decoded. The most well-known scenario that illustrates the basic idea of DNF is when the terminals use BPSK modulation in the MAC stage. Assume that the channel gains, H_A and H_B, are equal to 1 and the transmitted symbols from A and B are $X_A, X_B \in \{-1, 1\}$. The received signal at R is then $Y_R = X_A + X_B + Z_R$. If the MAC channel is noiseless, i.e., $Z_R = 0$, the possible received signals are $\{-2, 0, 2\}$. For the received signals -2 and 2, the relay can infer that the signal sent by the end nodes are $(X_A, X_B) = (-1, -1)$ and $(X_A, X_B) = (1, 1)$, respectively. However, if the relay R receives 0, there is an ambiguity whether the signals sent are $(X_A, X_B) = (-1, 1)$ or $(X_A, X_B) = (1, -1)$. But, for example, if A sends 1 and knows that the relay R has observed 0, then A can infer that $X_B = -1$. The relay node only needs to send one bit of information to assist A and B communication using the following denoising map: If it receives -2 or 2, it sends 1 in the BC stage, while it broadcasts -1 otherwise. One can easily check that, with the knowledge of X_A and X_R, A can infer X_B and, vice versa, knowing X_B and X_R, B can infer X_A. If the channel at R is noisy, then R needs to set appropriate decision regions to detect the symbols. The output of the decision process is a symbol from the set $\{-2, 0, 2\}$ and in the next step R applies the denoise mapping in order to compress the ternary symbol from the decision process to a binary symbol $\{-1, 1\}$ that needs to be sent in the broadcast phase. Overall, in order to implement a DNF scheme, the relay node R should (1) quantize the received signal using the appropriate decision regions and (2) map of the quantized signal to a symbol to be sent in the broadcast phase. For successful decoding, any arbitrary mapping $\mathcal{C}$, used at the relay R, should meet the

following requirements [23].

$$\mathcal{C}(s_1, s_2) \neq \mathcal{C}(s_1', s_2), \forall s_1 \neq s_1', s_2 \in \mathbb{F}$$
$$\mathcal{C}(s_1, s_2) \neq \mathcal{C}(s_1, s_2'), \forall s_2 \neq s_2', s_1 \in \mathbb{F} \qquad (2.7)$$

which is known as *exclusive-law* [23]. For binary, the most well-known denoising map is the XOR or equivalently modulo-2 addition:

$$\mathcal{C}(S_A, S_B) = S_A \oplus S_B = S_A + S_B \ (mod\ 2). \qquad (2.8)$$

2.2.3 Compress-and-Forward (CF)

Compress-and-forward (CF) is an interesting variant of the DNF schemes, in which the quantization/compression framework is used to determine the operations carried out at the relay node R. In CF scheme, first proposed in [32], after observing Y_R, the relay obtain its quantized version $\hat{Y}_R$ as well as the message S_R which is uniquely associated with $\hat{Y}_R$ and forwards it to the end nodes via X_R. To illustrate the decoding scheme, consider the decoder at node A which wishes to decode the relay message S_R in order to ultimately decode its intended message from node B, S_B. After the BC stage, node A has the known sequences X_A and Y_A and finds the set of all $\hat{Y}_R$ and X_R such that $(X_A, \hat{Y}_R)$ and (X_R, Y_A) are two pairs of jointly typical sequences. Then node A decodes S_R correctly if there exists a unique S_R for which both $(X_A, \hat{Y}_R)$ and (X_R, Y_A) are jointly typical sequences and declares a decoding error otherwise [33].

2.2.4 Compute-and-Forward

Compute-and-forward schemes are those where the relay decodes linear combination of the transmitted messages using the noisy linear combinations provided by the channel. Given enough linear combinations, an end node can solve for its desired messages. A compute-and-forward scheme relies on codes with a linear structure and was originally proposed in [18] for nested lattice codes. The linearity of the codebook ensures that linear combinations of codewords are themselves codewords. The relay can choose which linear equation to recover.

This strategy affords protection against noise as well as the opportunity to exploit interference for cooperative gains. Compared to amplify-and-forward and compress-and-forward in which a set of noisy linear equations is broadcasted by the relay, in this case, the relay forwards a set of reliable linear equations.

In this thesis, we propose a compute-and-forward type strategy in which linear functions of the transmitted messages over small fields are inferred from the noisy superimposed packets received at the relay. The linear coding schemes here are RS-CC and LDPC codes over small non-binary fields. RS-CC and LDPC codes are suitable for fast fading channels. For binary, the only linear function of the transmitted messages is the modulo-2 addition, which as explained in [23], does not offer the best probability of error performance for many channel conditions. For non-binary, however, there are multiple linear functions of the transmitted messages, i.e., network-coded combinations, to be decoded at the relay. Decoding multiple network-coded combinations can be helpful, since for a successful detection at the relay only one of these combinations needs to be successfully decoded. In other words, working over non-binary fields gives the relay node R the opportunity to map the received signal, Y_R, into multiple network-coded combinations; i.e., $S_R = aS_A + bS_B$ over $\mathbb{F}$, where $a, b \in \mathbb{F}\backslash\{0\}$.

2.3 Physical Layer Network Coding Over Non-Binary Fields

An advantage of working over non-binary fields is that it offers a variety of choices for the decoding coefficients. Decoding coefficients a and b can be selected from the set $\mathbb{F}\backslash\{0\}$. Decoding according to a fixed choice (a, b) partitions the q^2 received constellation points into q sets according to the level sets of the function of S_A and S_B, $\mathcal{C}_{(a,b)}(S_A, S_B) := aS_A + bS_B$ over $\mathbb{F}$. However, not all of these sets of decoding coefficients lead to a new partitioning of constellation points and thus do not provide a new opportunity for successful decoding at the relay. Those that generate the same partitioning of points either all succeed or all fail when decoding a particular received constellation. The following theorem indicates which of the coefficient pairs, (a, b), are not duplicates in this sense.

Theorem 1. *The number of distinct sets of decoding coefficients equals to $|\mathbb{F}| - 1$. Picking the coefficient $a = 1$ and $b \in \mathbb{F}\backslash\{0\}$ yields all the distinct sets.*

Proof. The proof consists of two parts: (1) any set of decoding coefficients, (a, b), where $a, b \in \mathbb{F}\backslash\{0\}$ and $a \neq 1$ is a duplicate of a set $(1, b')$, where $b' \in \mathbb{F}\backslash\{0\}$ and (2) there are no duplicate sets with an identical first coefficient.

Part 1: The partition with $(1, b)$, where $b \in \mathbb{F}\backslash\{0\}$, is the same as that with (k, kb), where $k \in \mathbb{F}\backslash\{0\}$, since

$$k\mathcal{C}_{(1,b)}(S_A, S_B) = kS_A + kbS_B = \mathcal{C}_{(k,kb)}(S_A, S_B), \tag{2.9}$$

i.e., decoding coefficients $(1, b)$ and (k, kb) produce the same partitioning.

As an example, consider working over $GF(3)$ field. The mapping from $Y_R \in \mathbb{C}$ back to $\mathbb{F} = \{0, 1, 2\}$ at the relay depends on the choice of (a, b). Fig. 2.1 illustrates mappings due to decoding coefficients $(1, 1)$ and $(2, 2)$, with constellation points labeled by (S_A, S_B). As can be seen from Fig. 2.1, the partitioning generated by $(1, 1)$ and $(2, 2)$ is the same. However, the level sets of $\mathcal{C}_{(1,1)}(S_A, S_B)$ are not identical as those of $\mathcal{C}_{(2,2)}(S_A, S_B)$.
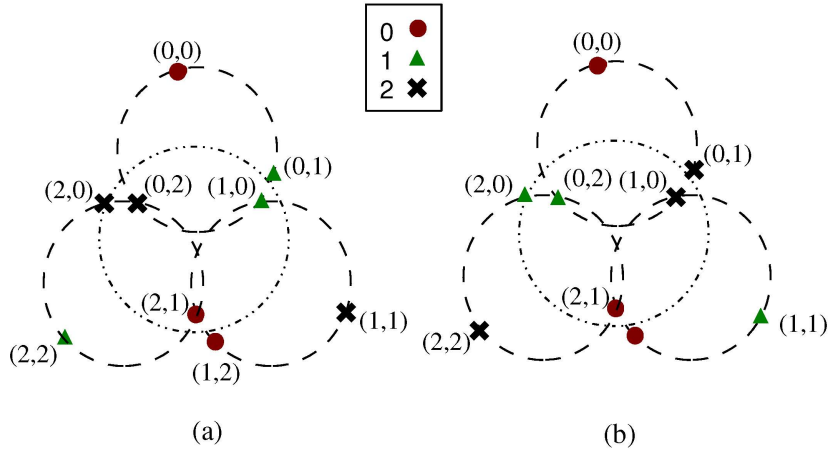

Figure 2.1: When working over $GF(3)$ field, mapping due to decoding coefficients $(1, 1)$ and $(2, 2)$ generate the same partitioning of the received constellation points at the relay: (a) $(a, b) = (1, 1)$, (b) $(a, b) = (2, 2)$

Part 2: Assume that the partition with $(1, b)$ is the same as that with $(1, b')$. Denote by $P \subset \mathbb{F}^2$ the common level set $\mathcal{K} \in \mathbb{F}$ and $\mathcal{K}' \in \mathbb{F}$ for $(1, b)$ and $(1, b')$, respectively, i.e., for all $(S_A, S_B) \in P$,

$$S_A + bS_B = \mathcal{K}$$
$$S_A + b'S_B = \mathcal{K}'. \tag{2.10}$$

According to (2.10), $(b' - b)S_B = \mathcal{K} - \mathcal{K}'$ for all S_B in $\{S | (S_A, S) \in P\} = \mathbb{F}$. But, this will only hold if $b = b'$ and $\mathcal{K} = \mathcal{K}'$. Therefore, there are no duplicate sets with an identical first coefficient. $\qquad\square$

In this thesis, the relay R performs soft-decision decoding to estimate S_R from the

received signal, Y_R, using the probability $\Pr(Y_R | aS_A + bS_B = k)$ for $k \in \mathbb{F}$, as follows

$$
\begin{aligned}
&\Pr(Y_R | aS_A + bS_B = k) \\
&= \frac{1}{|\mathbb{F}|} \sum_{S_A} \Pr(Y_R | aS_A + bS_B = k, S_A) \\
&= \frac{1}{|\mathbb{F}|\pi\sigma^2} \sum_{\substack{(S_A, S_B) \\ aS_A + bS_B = k}} \exp\left(\frac{-|Y_R - H_A \mathcal{M}(S_A) - H_B \mathcal{M}(S_B)|^2}{\sigma^2} \right).
\end{aligned}
\tag{2.11}
$$

2.4 Broadcast (BC) Stage

In the BC stage where the network-coded signal is broadcasted to nodes A and B, the received signal at the end node is written as

$$
Y_i = H_i X_R + Z_i, \text{ for } i \in \{A, B\},
\tag{2.12}
$$

where Z_i is complex-valued AWGN with a variance of σ^2 and H_i is complex-valued channel gain from the relay node R to the end nodes. Due to (2.7), end node A can extract the desired data S_B, using self-information as follows

$$
\hat{S}_A = \operatorname*{argmin}_{s \in \mathbb{F}} |Y_A - H_A \mathcal{M}(\mathcal{C}(S_A, s))|.
\tag{2.13}
$$

Analogously, the end node B detects the desired data S_A.

Chapter 3

Probability of Un-Encoded Error Performance

The Euclidean distance between any two constellation points belonging to different level sets of $\mathcal{C}_{(a,b)}$, i.e., $\mathcal{C}_{(a,b)}(S_A, S_B) \neq \mathcal{C}_{(a,b)}(S'_A, S'_B)$, is written as

$$d_{(S_A, S_B) - (S'_A, S'_B)} = |H_A||\Delta(S_A, S'_A) + \gamma e^{j\theta} \Delta(S_B, S'_B)|, \tag{3.1}$$

where $\Delta(s, s') = \mathcal{M}(s) - \mathcal{M}(s')$ and $H_B/H_A = \gamma e^{j\theta}$, where γ and θ are the channel amplitude ratio and the channel phase difference, respectively. Suppose that these two points are mistaken for one another, the pairwise error probability is given as

$$\Pr((S_A, S_B) \rightarrow (S'_A, S'_B)) = Q\left(\sqrt{\frac{d^2_{(S_A, S_B) - (S'_A, S'_B)}}{\sigma^2}}\right), \tag{3.2}$$

where $Q(.)$ represents the Q-function, the tail probability of the standard normal distribution. The total error is usually approximated by a weighted sum of all the pairwise error probabilities. The most dominant factor in this summation is the pairwise error probability corresponding to the minimum distance as follows

$$d_{min} = \min_{\substack{(S_A, S_B), (S'_A, S'_B) \\ \mathcal{C}_{(a,b)}(S_A, S_B) \neq \mathcal{C}_{(a,b)}(S'_A, S'_B)}} d_{(S_A, S_B) - (S'_A, S'_B)}. \tag{3.3}$$

3.1 Received Constellation Points at the Relay

We consider the received constellation points $\mathbf{M}_{\mathcal{M}}(H_A, H_B)$ at the relay. The explanations in this and the following section are for the case where the end nodes A and B use 3-PSK modulation; i.e, $S_A, S_B \in GF(3)$. Higher order constellations, however, are similar. In this case, decoding coefficients (a, b) can either be $(1, 1)$ or $(1, 2)$, owing to *Theorem* 1.
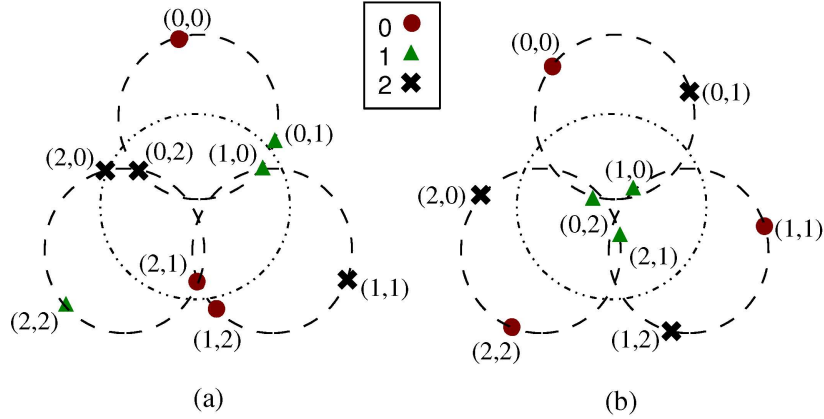

Figure 3.1: The received constellation points $\mathbf{M}_{\mathcal{M}}(H_A, H_B)$, mapped due to different decoding coefficients (a, b), when 3-PSK is used at the MAC stage: (a) $(a, b) = (1, 1)$, (b) $(a, b) = (1, 2)$

Fig. 3.1 illustrates the mappings from $Y_R \in \mathbb{C}$ back to $\mathbb{F} = \{0, 1, 2\}$ due to decoding coefficients $(1, 1)$ and $(1, 2)$, with constellation points labeled by (S_A, S_B). It is interesting to note that in Fig. 3.1(a), for $(a, b) = (1, 1)$, points at the periphery of the received constellation are mapped back to the same elements in $\mathbb{F}$, i.e.,

$$\mathcal{C}_{(1,1)}(1, 2) = \mathcal{C}_{(1,1)}(2, 1) = 0$$
$$\mathcal{C}_{(1,1)}(0, 1) = \mathcal{C}_{(1,1)}(1, 0) = 1$$
$$\mathcal{C}_{(1,1)}(0, 2) = \mathcal{C}_{(1,1)}(2, 0) = 2, \tag{3.4}$$

while in Fig. 3.1(b), for $(a, b) = (1, 2)$, it is points in the interior of the received constellation that are mapped to the same element in $\mathbb{F}$, i.e.,

$$\mathcal{C}_{(1,2)}(1, 0) = \mathcal{C}_{(1,2)}(2, 1) = \mathcal{C}_{(1,2)}(0, 2). \tag{3.5}$$

Thus, decodings with $(1, 1)$ and $(1, 2)$ result in different types of errors and attempting to decode against both can reduce the probability of error. Depending on which constellation points, S_A and S_B, are sent, one of these mappings has a better minimum distance and hence may improve the probability of error.

3.2 Minimum Distance

Decoding against both coefficient sets $(1, 1)$ and $(1, 2)$ prevents an arbitrary received constellation point such as $(1, 1)$ from being mistaken with either of the points: $(2, 2)$, $(0, 0)$, $(0, 2)$, or $(2, 0)$. The four remaining constellation points at the relay are: $(1, 0)$, $(1, 2)$, $(0, 1)$, and $(2, 1)$. The first two points are of distance $\sqrt{3}|H_B|$ from the point $(1, 1)$, where $|.|$ indicates taking the absolute value of the enclosed variable. The later two, however, are of distance $\sqrt{3}|H_A|$ from the point $(1, 1)$. Therefore, d_{min} assuming both decodings are attempted is

$$d_{min} = \sqrt{3} \min \left(|H_A|, |H_B| \right). \tag{3.6}$$

This is the distance between the initial set of constellation points times $\min(H_A, H_B)$. The same reasoning is valid for higher order constellations. Similarly, for higher order constellations, d_{min} equals the distance between the constellation points at the MAC stage times $\min(H_A, H_B)$. Generally, for higher order constellations, it can be shown that

$$d_{min} = \sqrt{2 \left(1 - \cos \left(\frac{2\pi}{q} \right) \right)} \min \left(|H_A|, |H_B| \right), \tag{3.7}$$

which is a decreasing function of q. Note that by decoding against all choices of coefficient sets (a, b), the value of d_{min} is independent of the channel phase difference, θ.

3.3 Comparing Probability of Error Performance

We assume independent Rayleigh-fading for channels from the end nodes A and B to the relay as follow

$$|H_i| \sim \mathcal{R} \left(\frac{1}{\sqrt{2}} \right), \text{ for } i \in \{A, B\} \tag{3.8}$$

The probability density function (pdf) of $H = \min(|H_A|, |H_B|)$ is obtained as,

$$f_H(h) = 4he^{-2h^2}, \ h \geq 0 \tag{3.9}$$

According to (3.2), d_{min} can be written as KH, where K is a constant. If the end nodes adopt binary constellation, each member of the received constellation at the relay is of distance d_{min} from one other point. On the other hand, in non-binary cases, any received signal point at the relay is of distance d_{min} from two other points. Therefore, the symbol error rate (SER) can be estimated with $K_q \mathbb{E}_H \left(Q \left(\sqrt{\frac{\log_2(q) \, d_{min}^2}{\sigma^2}} \right) \right)$, where $\mathbb{E}_H(.)$ indicates taking the expected value of the enclosed variable with respect to $f_H(h)$ and K_q equals to 1 for the binary case and equals to 2 otherwise, as follows

$$
\begin{aligned}
SER &= K_q \int_0^\infty 4he^{-2h^2} Q\left(\sqrt{\frac{\log_2(q)\, d_{min}^2}{\sigma^2}}\right) dh \\
&= K_q \int_0^\infty 4he^{-2h^2} Q\left(\sqrt{\frac{\log_2(q)\, K^2 h^2}{\sigma^2}}\right) dh \\
&= \frac{K_q}{2} \int_0^\infty e^{\frac{-l}{2}} Q\left(\sqrt{\frac{\log_2(q)\, K^2 l}{4\sigma^2}}\right) dl \\
&= \frac{K_q}{2} \int_0^\infty e^{\frac{-l}{2}} \frac{1}{\sqrt{2\pi}} \int_{\sqrt{\frac{\log_2(q)\, K^2 l}{4\sigma^2}}}^\infty e^{\frac{-u^2}{2}} du \ dl \\
&= \frac{K_q}{2\sqrt{2\pi}} \int_0^\infty e^{\frac{-u^2}{2}} \int_0^{\frac{4\sigma^2 u^2}{\log_2(q)\, K^2}} e^{\frac{-l}{2}} dl \ du \\
&= \frac{K_q}{2\sqrt{2\pi}} \int_0^\infty e^{\frac{-u^2}{2}} \, 2\left(1 - e^{\frac{-2\sigma^2 u^2}{\log_2(q)\, K^2}}\right) du \\
&= K_q \left(1 - \frac{1}{\sqrt{2\pi}} \int_0^\infty e^{\frac{-u^2}{2}\left(1 + \frac{4\sigma^2}{\log_2(q)\, K^2}\right)} du\right) \\
&= K_q \left(1 - \frac{1}{\sqrt{1 + \frac{4\sigma^2}{\log_2(q)\, K^2}}}\right). \tag{3.10}
\end{aligned}
$$

And hence, the SER performance follows as

$$SER = K_q \left(1 - \frac{1}{\sqrt{1 + \frac{2\sigma^2}{(1 - cos(2\pi/q)) \log_2(q)}}} \right) \quad K_q = \begin{cases} 1 & \text{for} & \mathbb{F} = GF(2) \\ 2 & \text{for} & \text{other wise} \end{cases} \qquad (3.11)$$
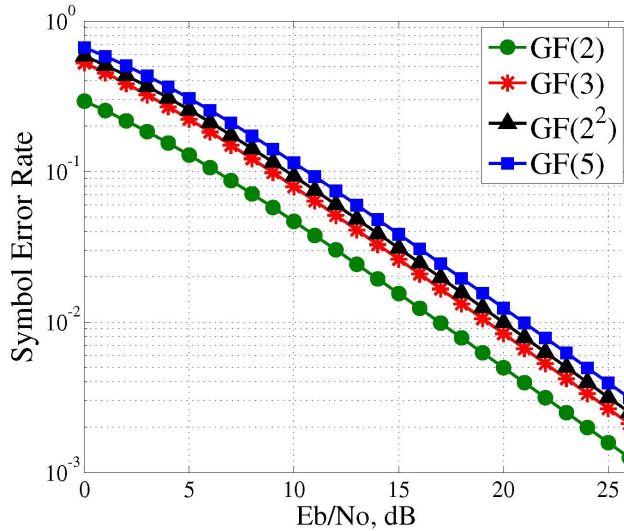

Figure 3.2: Un-encoded symbol error rate for binary and non-binary constellations

Fig. 3.2 illustrates the approximate SER vs. E_b/N_0 for different fields. As can be seen from Fig. 3.2, un-encoded SER of the binary case is less than that of the non-binary constellations. However, the SER can be misleading, since, for instance, in 64-QAM, each symbol is 6-bit long. Even if each symbol had one of its six bits in error, a symbol error rate of 100% has occurred, yet simple error correction schemes could correct each erroneous bit. Thus, a more appropriate basis for comparison is the FER with coding rather than un-encoded SER.

Chapter 4

Channel Coded Bidirectional Relaying

We let $\mathcal{T} : \mathbb{F}^k \to \mathbb{F}^n$ denote a linear channel encoder. Denote by $\mathbf{S}_A$ and $\mathbf{S}_B$ the unencoded data to be transmitted from A and B, where $\mathbf{S}_A, \mathbf{S}_B \in \mathbb{F}^k$. The end nodes employ a coding scheme of rate $r = k/n$. The encoded packets are then modulated by $\mathcal{M} : \mathbb{F}^n \to \mathbb{C}^n$, the PSK constellation mapper, as

$$\mathbf{X}_A = \mathcal{M}\left(\mathcal{T}(\mathbf{S}_A)\right)$$
$$\mathbf{X}_B = \mathcal{M}\left(\mathcal{T}(\mathbf{S}_B)\right). \tag{4.1}$$

Let $\mathbf{U}_A = \mathcal{T}(\mathbf{S}_A)$ and $\mathbf{U}_B = \mathcal{T}(\mathbf{S}_B)$ denote the encoded packets from the end nodes. In the MAC stage, the received signal at the relay node R during the j-th symbol is written as

$$Y_R(j) = H_A(j)X_A(j) + H_B(j)X_B(j) + Z_R(j), \tag{4.2}$$

where $Z_R(j)$ is complex-valued circularly symmetric AWGN with variance σ^2 and $H_i(j)$ for $i \in \{A, B\}$ is a complex-valued channel gain from the end node i to the relay node R. In this thesis, we first consider quasi-static fading channels, where $H_i(j)$ is a constant for all $j \in \{1, 2, ..., n\}$. When we consider fast fading channels, the $H_i(j)$ are assumed to be i.i.d. for all $j \in \{1, 2, ..., n\}$.

We aim to directly decode $a\mathbf{S}_A + b\mathbf{S}_B$ over $\mathbb{F}$, using the fact that $\mathcal{T} : \mathbb{F}^k \to \mathbb{F}^n$ is a linear code. The linearity of the code guarantees that adding any two code words

produces another code word, i.e.,

$$\mathcal{T}(a\mathbf{S}_A + b\mathbf{S}_B) = a\mathcal{T}(\mathbf{S}_A) + b\mathcal{T}(\mathbf{S}_B). \tag{4.3}$$

Therefore, if from $\mathbf{Y}_R$ we can obtain the soft metrics $\Pr(Y_R(j)|aS_A(j) + bS_b(j))$ for $j \in \mathbb{Z}_n$, according to (2.11) and the linear code allows for soft-input decoding, we can directly decode $a\mathbf{S}_A + b\mathbf{S}_B$ without first decoding $\mathbf{S}_A$ and $\mathbf{S}_B$. Moreover, we assume that the BC stage is fairly standard, as explained in 2.4.

4.1 Review of the Coding Schemes

In this section, we present a short review of different linear channel coding schemes used in this thesis.

4.1.1 Reed-Solomon Convolutional Code Concatenation

Code concatenation first proposed by Forney in [34] is an error correcting scheme in which two different error correcting codes called the inner code and outer code are concatenated, achieving comparatively higher coding gain by using codes that are relatively easy to decode. It is well-known, that the concatenation of two channel codes leads to a more robust code [35]. The concatenated coding scheme using convolutional coding (CC) with Viterbi decoding as the inner code and the Reed-Solomon (RS) code as the outer code is a special case of the general concatenated coding scheme proposed by Forney.

Convolutional Codes

Convolutional codes can be specified as $CC(n, k, m)$, where n is the number of output bits, k is the number of input bits, m is the number of memory registers, and the ratio $r = n/k$ called the code rate, is a measure of the efficiency of the code. In convolutional code, each transformation is a function of the previous $L = k(m - 1)$ information symbols, where L is called the constraint length of the code. In other words, the constraint length L represents the number of symbols in the encoder memory that affect the generation of the n output symbols. The decoding algorithm used in this thesis is Viterbi with soft-decision inputs.

Convolutional codes are used widely in numerous applications in order to achieve reliable data transfer, including digital video, radio, mobile communication, and satellite

communication. These codes are often implemented in concatenation with a hard-decision code, especially Reed-Solomon, as in this thesis. For a complete survey on convolutional codes, refer to [35].

Reed-Solomon Codes

A $RS(n, k, m)$ code is used to encode k, m-symbol blocks into $n \leq q^m - 1$ blocks consisting of m symbols, as shown in Fig. 4.1. The encoder thus consists of $m \times k$ input symbols and $m \times n$ output symbols. Also,
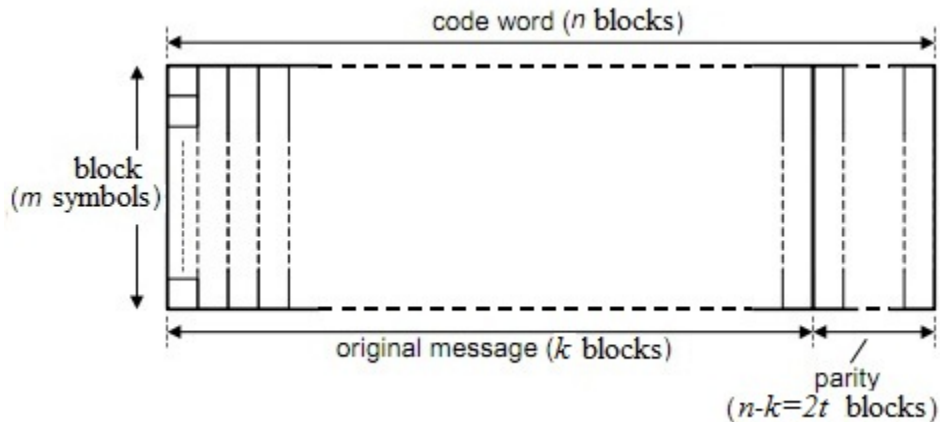
$$n \leq 2^m - 1. \tag{4.4}$$

Figure 4.1: Reed-Solomon code definitions

When (4.4) is not an equality, RS is referred to as a shortened code. There are $n - k$ parity block and t block errors can be corrected in a codeword, where

$$t = \begin{cases} \frac{n-k}{2} & \text{for } n - k \text{ even} \\ \frac{n-k-1}{2} & \text{for } n - k \text{ odd} \end{cases} \tag{4.5}$$

RS codes are not only linear, but also they are cyclic, which means that cyclically shifting the symbols of a codeword produces another codeword. While RS code belongs to the family of BCH codes, it is distinguished by having multi-symbol blocks. RS codes are known to be good at dealing with bursts of errors, since although a block may have

all its symbols in error, this counts as only one block error in terms of the correction capacity of the code.

Reed-Solomon codes were developed in 1960 by Irving S. Reed and Gustave Solomon [36]. When the article was written, no efficient decoding algorithm was known. A decoding solution was found in 1969 by Elwyn Berlekamp and James Massey, and is since known as the Berlekamp-Massey decoding algorithm. This is the decoding algorithm employed in this thesis. In 1977, RS codes were implemented in the Voyager program in the form of concatenated codes. The first commercial application in mass-production appeared in 1982 with the compact disc, where two interleaved RS codes were utilized. Today, RS codes are extensively used in digital storage devices and digital communication standards, however they are being gradually replaced by more modern codes such as low density parity check codes or turbo codes. For instance, RS codes are used in the digital video broadcasting (DVB) standard DVB-S, but LDPC codes are now used in its successor DVB-S2.

4.1.2   Low Density Parity Check (LDPC)

As the terminology suggests, LDPC codes, also known as Gallager codes [37], are constructed using sparse bipartite graphs. LDPC codes can be specified by (n, m) parameters, where n is the number of non-zero elements in the columns and m is that in the rows. LDPC codes are shown to have near-Shannon performance [38], which means that practical constructions exist that allow the noise threshold to be set very close to the Shannon limit for a symmetric memory less channel. The belief propagation decoding method first proposed by Gallager has been further improved and generalized by many research groups. Davey and MacKay [39] have introduced a generalized decoding technique that can be applied to non-binary codes as well. They have shown that the near-Shannon limit performance of Gallager's binary low density parity check code can be significantly enhanced by moving to fields of higher order. In this thesis, we implement the decoding algorithm introduced in [39].

In a bipartite graph any even-length path of edges finishes in the same set it started, and an odd-length path finishes in the opposite set. A loop is a closed path of even length in which the first node is the same as the last one. Since there is at most one edge between any two nodes, the shortest length a loop can have is 4, the next largest is 6, and so on. The *girth* of a graph is the length of its shortest loop. If the graph contains no loops then the decoding is quickly computable. Since decoding methods of the LDPC codes are iterative, the main problem of a loopy graph is that the value of an incorrect node in a loop will propagate back to itself, resisting the efforts of the algorithm to correct it. Longer loops, however, dilute this effect and are not as critical

to the decoders performance. Therefore, many efforts have been made for detecting and removing loops from LDPC graphs [40, 41].

LDPC codes are finding increasing use in applications where reliable and highly efficient information transmission over bandwidth in the presence of noise is desired. In 2003, an LDPC code beat six turbo codes and became the error correcting code in the DVB-S2 standard for the satellite transmission of digital television. In 2008, an LDPC code beat convolutional turbo codes as the forward error correction (FEC) scheme for the ITU-T G.hn standard. Because of its low decoding complexity, specifically when operating at data rates close to 1 Gbit/s, G.hn chose LDPC over turbo codes. Also, 10GBase-T Ethernet, which sends data at 10 Gbit/s over twisted-pair cables, uses LDPC codes. In 2009, LDPC codes became a part of the Wi-Fi 802.11 standard, as an optional part of 802.11n, in the high throughput physical layer specification.

Chapter 5

q-PSK Constellation Mappers

Working over larger fields provides different choices for constellation mappers. Generally, in a field of size q, there are $q!$ different constellation mappers that place the constellation points uniquely on a q-PSK constellation. However, due to symmetric properties of the constellation and the fact that linear codes are employed at the end nodes, the number of constellation mappers with different performance in terms of FER, called *distinct mappers* for short, is less. Consider a constellation mapper $\mathcal{M}$ that generates the constellation $\mathbf{c}_1 = (c_{11}, c_{12}, ..., c_{1q})$, where $c_{1i} \in \mathbb{F}$, $c_{1i} \neq c_{1j}$ for $i \neq j$ and $i, j \in \{1, 2, ..., q\}$, with a given FER; without loss of generality, let c_{11} be located at the right corner of the q-PSK constellation, followed by $c_{12}, ..., c_{1q}$ in a counter-clockwise order. The constellation $\mathbf{c}_1$ can be transformed to another constellation called $\mathbf{c}_2 = (c_{21}, c_{22}, ..., c_{2q})$, where $c_{2i} \in \mathbb{F}$, $c_{2i} \neq c_{2j}$ for $i \neq j$ and $i, j \in \{1, 2, ..., q\}$, by applying a permutation such as rotation, or reflection, etc. Since the total number of permutations is $q!$, there exists $q!$ different constellations. Let us denote by $\mathcal{P} = \{p_i | 1 \leq i \leq q!\}$ the group of all $q!$ permutations. Without loss of generality assume that the elements of $\mathbb{F}$ are ordered as $\{\xi_1, \xi_2, ...\xi_q\}$. Denote by $\mathcal{C} = \{\mathbf{c}_i | 1 \leq i \leq q!\}$ the set of all constellations created by applying the elements of $\mathcal{P}$ to $\mathbf{c}_I = (\xi_1, \xi_2, ..., \xi_q)$, an *identity constellation*. Since there is a one-to-one correspondence between the elements of $\mathcal{C}$ and those of $\mathcal{P}$, there exists an isomorphism between $\mathcal{P}$ and $\mathcal{C}$ and hence $\mathcal{C}$ can be seen to have group structure. In the following, we investigate the permutations of the constellation $\mathbf{c}_1$ that result in the same FER performance as $\mathbf{c}_1$: rotation, reflection, and multiplication by non-zero field elements.

5.1 Rotation

Now, consider the $q - 1$ constellations obtained by rotating the constellation points of $\mathbf{c}_1$ by $2k\pi/q$ for $k \in \mathbb{Z}_q\backslash\{0\}$. If instead of $\mathcal{M}$ the constellation mapper $\mathcal{M}' : \mathbb{F} \to \mathbb{C}$ that is equivalent to a $2k\pi/q$ rotation of the constellation induced by $\mathcal{M}$ is used, then the received constellation at the j-th time instant $\mathbf{M}_{\mathcal{M}'}(H_A(j), H_B(j))$ is identical to $\mathbf{M}_{\mathcal{M}}(H_A(j)e^{i2k\pi/q}, H_B(j)e^{i2k\pi/q})$. Since for Rayleigh fading the effect of the channel includes a random rotation uniform on $[0, 2\pi)$, the sets of possible received constellations $\mathbf{M}_{\mathcal{M}}(H_A(j), H_B(j))$ and $\mathbf{M}_{\mathcal{M}'}(H_A(j), H_B(j))$ have the same distribution. Therefore, any rotation of $\mathbf{c}_1$ has the same FER as $\mathbf{c}_1$.

5.2 Reflection

Also consider the constellation obtained by reflecting the constellation points of $\mathbf{c}_1$ on the x-axis. Let us denote by $\mathcal{M}' : \mathbb{F} \to \mathbb{C}$ the constellation mapper that is equivalent to the reflection of the constellation induced by $\mathcal{M}$ on the x-axis. Note that if $X_{c_{1j}}$, $j \in \{1, 2, ..., q\}$ is the coordinate of the point c_{1j} in the constellation $\mathbf{c}_1$, then, after the reflection, the point c_{ij} is located in the coordination $X_{c_{ij}}^*$, where the * indicates complex conjugate. At the j-th time instant, the received constellation points in $\mathbf{M}_{\mathcal{M}'}(H_A(j), H_B(j))$ are a reflection of those in $\mathbf{M}_{\mathcal{M}}(H_A(j)^*, H_B(j)^*)$ on the x-axis, as follows

$$
\begin{aligned}
&\mathbf{M}_{\mathcal{M}'}(H_A(j), H_B(j)) \\
&= \{H_A(j)\mathcal{M}'(S_A(j)) + H_B(j)\mathcal{M}'(S_B(j)) | S_A(j), S_B(j) \in \mathbb{F}\} \\
&= \{(H_A(j)^*\mathcal{M}(S_A(j)) + H_B(j)^*\mathcal{M}(S_B(j)))^* | S_A(j), S_B(j) \in \mathbb{F}\} \quad (5.1)
\end{aligned}
$$

Since the added noise is complex-valued circularly symmetric AWGN, the reflection permutation does not change its distribution. Also, since for Rayleigh fading the probability distribution of $H_i(j)$ and $H_i(j)^*$, for $i \in \{A, B\}$, is the same, the sets of possible received constellations $\mathbf{M}_{\mathcal{M}}(H_A(j), H_B(j))$ and $\mathbf{M}_{\mathcal{M}'}(H_A(j), H_B(j))$ have an identical distribution and hence, a reflection of $\mathbf{c}_1$ has the same FER as $\mathbf{c}_1$.

5.3 Multiplication by Non-Zero Field Elements

Knowing that $\mathbf{S}_A$ and $\mathbf{S}_B$ are selected uniformly and iid on $\mathbb{F}^k$, encoding and transmitting $c\mathbf{S}_A$ and $c\mathbf{S}_B$ for $c \in \mathbb{F}\backslash\{0\}$ has the same FER performance as encoding and transmitting

$\mathbf{S}_A$ and $\mathbf{S}_B$ if a linear code is used. This is because for $c = 1$, nothing has changed, while for $c \in \mathbb{F}\backslash\{0, 1\}$, we still have independent uniform distributions on $\mathbb{F}^k$. But compared to $c = 1$, the effect of using $c \in \mathbb{F}\backslash\{0, 1\}$ is as if we encoded using $c = 1$, and simply adopting the constellation $\mathbf{c}_2 = c\mathbf{c}_1 = (cc_{11}, cc_{12}, ..., cc_{1q})$ instead of $\mathbf{c}_1$ at the relay. Therefore, any constellation resulting from multiplication of $\mathbf{c}_1$ by $c \in \mathbb{F}\backslash\{0\}$ has the same FER as $\mathbf{c}_1$.

5.4 Number of Distinct Mappers

Let $H_1 \subset \mathcal{P}$ be the set of permutations corresponding to rotations and reflections of the constellation (these are left permutations); and $H_2 \subset \mathcal{P}$ the set of permutations corresponding to multiplications by non-zero field elements (these are right permutations). For $\mathbf{c}_1, \mathbf{c}_2 \in \mathcal{C}$, if $h_1\mathbf{c}_1h_2 = \mathbf{c}_2$, where $h_1 \in H_1$ and $h_2 \in H_2$, then $\mathbf{c}_1$ and $\mathbf{c}_2$ have the same performance in terms of FER and we say they are equivalent. The group $\mathcal{C}$ is thus divided into distinct classes of equivalent elements. If $\mathbf{c} \in \mathcal{C}$, we are interested in the double cosets $H_1\mathbf{c}H_2$ with respect to H_1 and H_2, as follows

$$H_1\mathbf{c}H_2 = \{h_1\mathbf{c}h_2 | h_1 \in H_1, h_2 \in H_2\}. \tag{5.2}$$

Thus, double cosets of H_1 and H_2 partition $\mathcal{C}$, where each partition consists of constellations with equivalent FER. The following theorem from [42] indicates the number of members in each partition, which in turn specifies the number of partitions and distinct mappers.

Theorem 2. *For a double coset $H_1\mathbf{c}H_2$ and $\mathbf{c} \in \mathcal{C}$, the number of members in the partition with $\mathbf{c}$ is equal to*

$$\#(H_1\mathbf{c}H_2) = \frac{|H_1||H_2|}{|H_1\mathbf{c} \cap \mathbf{c}H_2|}, \tag{5.3}$$

where $|.|$ indicates the size of the enclosed set. In the following, we investigate the number of distinct mappers for $GF(3)$, $GF(2^2)$, and $GF(5)$ fields, in detail.

For the case that $\mathbb{F} = GF(3)$, the group $\mathcal{C}$ has 6 elements and as $|H_1| = 6$, $\mathcal{C}$ has 1 partition. Thus even for non-linear coding schemes all 3! constellations have the same performance in terms of FER.

If $\mathbb{F} = GF(2^2)$, we have $|H_1| = 8$, $|H_2| = 3$, and $|H_1\mathbf{c} \cap \mathbf{c}H_2| = 1$ for all $\mathbf{c} \in \mathcal{C}$, and thus the group $\mathcal{C}$ will consist of one partition of size 24. Hence all 4! constellations
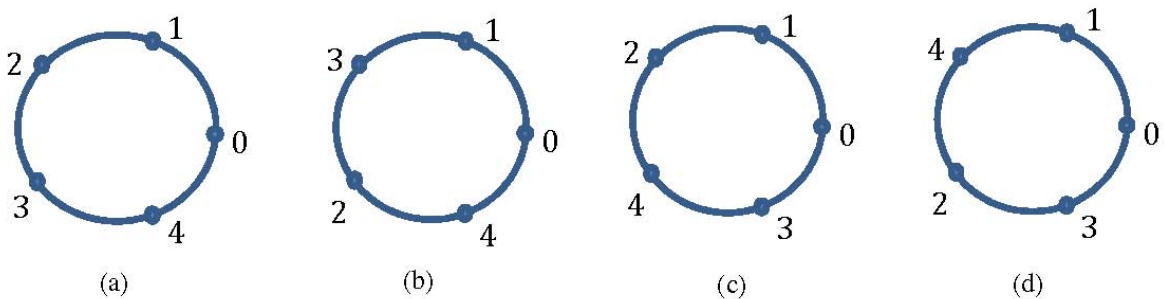
Figure 5.1: The four distinct constellations: (a) belongs to a partition of size 20, (b) belongs to a partition of size 20, (c) belongs to a partition of size 40, and (d) belongs to a partition of size 40.

have the same performance in terms of FER if a linear coding scheme is employed at the end nodes. If the code is non-linear, then the number of distinct mappers equals to $|H_2| = 3$.

Finally, if $\mathbb{F} = GF(5)$, we have $|H_1| = 10$, $|H_2| = 4$, and $|H_1\mathbf{c} \cap \mathbf{c}H_2| = 1$ or 2 depending on $\mathbf{c} \in \mathcal{C}$. Thus the group $\mathcal{C}$ will be partitioned into 4 groups: two of size 20, and two of size 40, which means that there are 4 distinct mappers if a linear code is employed. As a result, if linear coding is employed at the end nodes, only four distinct mappers should be considered as all others have identical performance in terms of FER. Fig. 5.1 depicts one member of each partition. Note that Fig. 5.1(a) and (b) show constellations that belong to partitions of size 20, while Fig. 5.1(c) and (d) show constellations that belong to partitions of size 40.

There are a number of examples that show the constellation mappers illustrated in Fig. 5.1 are in fact different in terms of FER. Since different minimum distances between the code words result in different FER performance, showing that there exits a linear code for which these constellations have different d_{min}, proves that they have different performances in terms of FER. For the linear code book $\mathcal{C}_1 : \mathbb{F} \rightarrow \mathbb{F}^4 = \{1234, 2413, 4321, 3142, 0000\}$, Table 5.1 illustrates the minimum distance between the code words for the configuration shown in Fig. 5.2.

For the linear code book $\mathcal{C}_2 : \mathbb{F}^2 \rightarrow \mathbb{F}^5 = \{$linear span of 11223 and 21344$\}$, Table 5.2 illustrates the minimum distance between the code words for the configuration shown in Fig. 5.2.

Therefore, code books $\mathcal{C}_1$ and $\mathcal{C}_2$ show that for linear codes the four constellation mappings shown in Fig. 5.1 might have different performances in terms of FER.
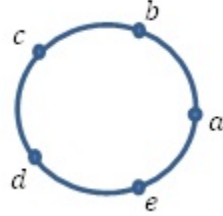
30

Figure 5.2: A 5-PSK mapper, where $a, b, c, d, e \in GF(5)$ are pairwise different.

Table 5.1: Minimum distance between the code words of the code $\mathcal{C}_1$ for the four distinct constellation mappings shown in Fig. 5.1

abcde	d_{min}
01234	3.1623
01324	3.1623
01243	2.7864
01342	2.3511

Table 5.2: Minimum distance between the code words of the code $\mathcal{C}_2$ for the four distinct constellation mappings shown in Fig. 5.1

abcde	d_{min}
01234	2.5263
01324	2.0361
01243	2.0361
01342	2.0361

31

Chapter 6

The Lower Bound on the FER Performance

In this section, we aim at finding a lower bound on the FER performance of encoded PNC for quasi-static fading channels. We denote by $\mathbf{S}_{AB} = a\mathbf{S}_A + b\mathbf{S}_B$ and $\mathbf{U}_{AB} = a\mathbf{U}_A + b\mathbf{U}_B$. Let us denote by $\mathcal{I} = I(\mathbf{Y}_R; \mathbf{S}_{AB}|H_A, H_B)$, the mutual information between the superimposed received signals at the relay node and the decoded network-coding combination, given the channel gains. As the source messages are selected according to a uniform distribution,

$$
\begin{aligned}
nr \log_2(q) &= \log_2(q^k) \\
&= h(\mathbf{S}_{AB}) \\
&= h(\mathbf{S}_{AB}|H_A, H_B) \\
&= I(\mathbf{S}_{AB}; \mathbf{Y}_R|H_A, H_B) + h(\mathbf{S}_{AB}|\mathbf{Y}_R, H_A, H_B) \\
&\leq \mathcal{I} + P_e nr \log_2(q) + 1 & (6.1) \\
&= \mathcal{I} + n\epsilon_n, & (6.2)
\end{aligned}
$$

where (6.1) follows from Fano's inequality, and $\epsilon_n \to 0$ as the probability of error $P_e \to 0$. According to (6.2) the probability of $\mathcal{I}$ being less than $nr \log_2(q)$ is an indicator of the probability of error, called *information outage probability*. We denote the information outage probability by $P_o = \Pr\{\mathcal{I} \leq nr \log_2(q)\}$.

There is a one-to-one relation between $\mathbf{S}_{AB}$ and U_{AB}, and thus $\mathcal{I} = I(\mathbf{Y}_R; \mathbf{U}_{AB}|H_A, H_B)$. For simplicity, in the following, we show $Y_R(j)$, $H_A(j)$, $H_B(j)$, $S_{AB}(j)$, $U_{AB}(j)$, $U_A(j)$,

and $U_B(j)$ for any time instant $j \in \{1, 2, ..n\}$ by Y_R, H_A, H_B, S_{AB}, U_{AB}, U_A, and U_B, respectively.

Now, assume a code of rate $r = k/n$ and, without loss of generality, that the first k symbols are systematic. Then the last $n - k$ symbols of $\mathbf{U}_A$ and $\mathbf{U}_B$ are dependent on the first k and hence the last $n - k$ symbols of $\mathbf{U}_{AB}$ are dependent to the first k. Let us denote the first k symbols of the received signal, by $\mathbf{Y}_R^{(1,k)}$ and the last $n - k$ by $\mathbf{Y}_R^{(k+1,n)}$. We denote the last $n - k$ symbols of the encoded packets by $U_A^{(k+1,n)}$ and $U_B^{(k+1,n)}$. The information $\mathcal{I}$ can then be rewritten as

$$
\begin{aligned}
\mathcal{I} &= h(\mathbf{Y}_R | H_A, H_B) - h(\mathbf{Y}_R | \mathbf{U}_{AB}, H_A, H_B) \\
&\le nh(Y_R | H_A, H_B) - h(\mathbf{Y}_R^{(1,k)} | \mathbf{U}_{AB}, H_A, H_B) \\
&\quad - h(\mathbf{Y}_R^{(k+1,n)} | \mathbf{Y}_R^{(1,k)}, \mathbf{U}_{AB}, H_A, H_B) \\
&\le nh(Y_R | H_A, H_B) - kh(Y_R | U_{AB}, H_A, H_B) \\
&\quad - h(\mathbf{Y}_R^{(k+1,n)} | \mathbf{Y}_R^{(1,k)}, \mathbf{U}_{AB}, \mathbf{U}_A^{(k+1,n)}, H_A, H_B) \\
&= nh(Y_R | H_A, H_B) - kh(Y_R | U_{AB}, H_A, H_B) \\
&\quad - h(\mathbf{Y}_R^{(k+1,n)} | \mathbf{Y}_R^{(1,k)}, \mathbf{U}_{AB}, \mathbf{U}_B^{(k+1,n)}, \mathbf{U}_A^{(k+1,n)}, H_A, H_B) \\
&= nh(Y_R | H_A, H_B) - kh(Y_R | U_{AB}, H_A, H_B) - (n - k)h(Z_R) \\
&= kI(Y_R; U_{AB} | H_A) + (n - k)I(Y_R; U_A, U_B | H_B).
\end{aligned}
$$

(6.3)

(6.4)

On the other hand, the information $\mathcal{I}$ can also be bounded by

$$
\begin{aligned}
\mathcal{I} &\le I(\mathbf{U}_{AB}; \mathbf{Y}_R, \mathbf{U}_A | H_A, H_B) \\
&= I(\mathbf{U}_{AB}; \mathbf{Y}_R | \mathbf{U}_A, H_A, H_B) \\
&= h(\mathbf{Y}_R | \mathbf{U}_A, H_A, H_B) - h(\mathbf{Y}_R | \mathbf{U}_{AB}, \mathbf{U}_A, H_A, H_B) \\
&\le nh(Y_R | U_A, H_A, H_B) - nh(Z_R) \\
&= nI(Y_R; U_B | U_A, H_A, H_B)
\end{aligned}
$$

(6.5)

(6.6)

Essentially, this is a bound on communicating from U_B to Y_R assuming U_A is known, and thus, its interference can be subtracted. Similarly,

$$
\mathcal{I} \le nI(Y; U_A | U_B, H_A, H_B).
$$

(6.7)

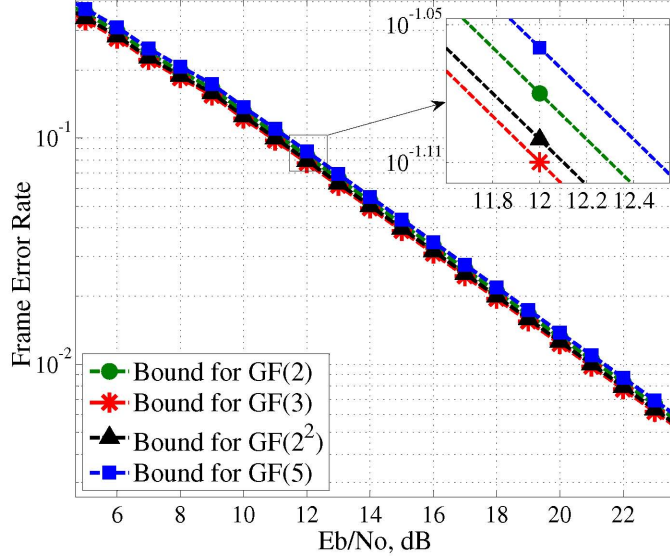Thus from (6.4), (6.6), and (6.7), the information outage probability is lower bounded

33

Figure 6.1: The lower bound on the FER performance of the encoded PNC

by

$$
\begin{aligned}
P_o > \Pr\{\min\{ & \\
& rI(Y_R; U_{AB}|H_A, H_B) + (1-r)I(Y_R; U_A, U_B|H_A, H_B), \\
& I(Y_R; U_B|U_A, H_A, H_B), \\
& I(Y_R; U_A|U_B, H_A, H_B)\} \leq r\log_2(q)\}.
\end{aligned}
\tag{6.8}
$$

We expect the bound in (6.4) to have diversity order two since,

$$
\begin{aligned}
& rI(Y_R; U_{AB}|H_A, H_B) + (1-r)I(Y_R; U_A, U_B|H_A, H_B) \\
& \geq (1-r)I(Y_R; U_A, U_B|H_A, H_B) \\
& \geq (1-r)I(U_A; Y_R|H_A, H_B) + (1-r)I(U_B; Y_R|U_A, H_A, H_B) \\
& \geq (1-r)I(U_B; H_B U_B + Z_R|H_B).
\end{aligned}
\tag{6.9}
$$

Analogously,

$$
\begin{aligned}
& rI(Y_R; U_{AB}|H_A, H_B) + (1-r)I(Y_R; U_A, U_B|H_A, H_B) \\
& \geq (1-r)I(U_A; H_A U_B + Z_R|H_A).
\end{aligned}
\tag{6.10}
$$

34

Hence,

$$rI(Y_R; U_{AB}|H_A, H_B) + (1-r)I(Y; U_A, U_B|H_A, H_B)$$
$$\geq (1-r)\max\{I(U_A; H_A U_A + Z_R|H_A), I(U_B; H_B U_B + Z_R|H_B)\}. \tag{6.11}$$

Therefore the information $I(Y_R; U_A, U_B|H_A, H_B)$ treats both U_A and U_B as desirable information, i.e., according to the received constellation points if just one of H_A or H_B is large, we will get about $\log_2(q)$ bits per channel use. So we need both H_A and H_B to be small for things to go wrong, which creates a slope of -20dB in FER vs. E_b/N_0. Since (6.4) has diversity order two, it does not affect the high SNR analysis however in low SNR regimes it helps to increase the lower bound.

Knowing that the steps in (6.3) and (6.5) are potentially loose, we expect the final bound (6.8) to be unrealizable, i.e., we do not expect any actual code to meet it in terms of FER performance. The bound (6.8), is depicted in Fig. 6.1. Also, note that the bound in (6.8) is valid for all $GF(5)$ distinct constellations shown in Fig. 5.1.

Chapter 7

Simulation Results

In this chapter, we compare the error performance of non-binary constellations in PNC with that of the binary case, in three different scenarios:

- without adopting any channel coding schemes

- by using practical RS-CC concatenation

- by using an LDPC code

The later two are investigated for both quasi-static and fast fading channels.

7.1   No Channel Coding

For the system configuration of Chapter 3, the simulation results of SER versus E_b/N_0 for the field $\mathbb{F} = GF(q)$, $(q = 2, 3, 4, 5)$ are shown in Fig. 7.1. As can be seen from Fig. 7.1, attempting to decode against all choices of decoding coefficients (a, b), improves the SER of the system in non-binary fields. However, this improvement can not compensate for the cost of the minimum distance reduction in non-binary fields, and hence the binary constellation outperforms the non-binary cases in the sense of minimizing the SER. In particular, the improvement obtained by decoding against multiple effective combinations is 0.6dB in E_b/N_0 for the field $GF(3)$ as shown in Fig. 7.1(a). From Fig. 7.1(b) and (c), the improvement gaps for both $GF(2^2)$ and $GF(5)$ fields are about 2dB in E_b/N_0. Fig. 7.1(d) illustrates the simulation results of SER performance for

binary and non-binary fields when attempting to decode against all choices of decoding coefficients (a, b). Note that these curves completely match the theoretical results shown in Fig. 3.2.
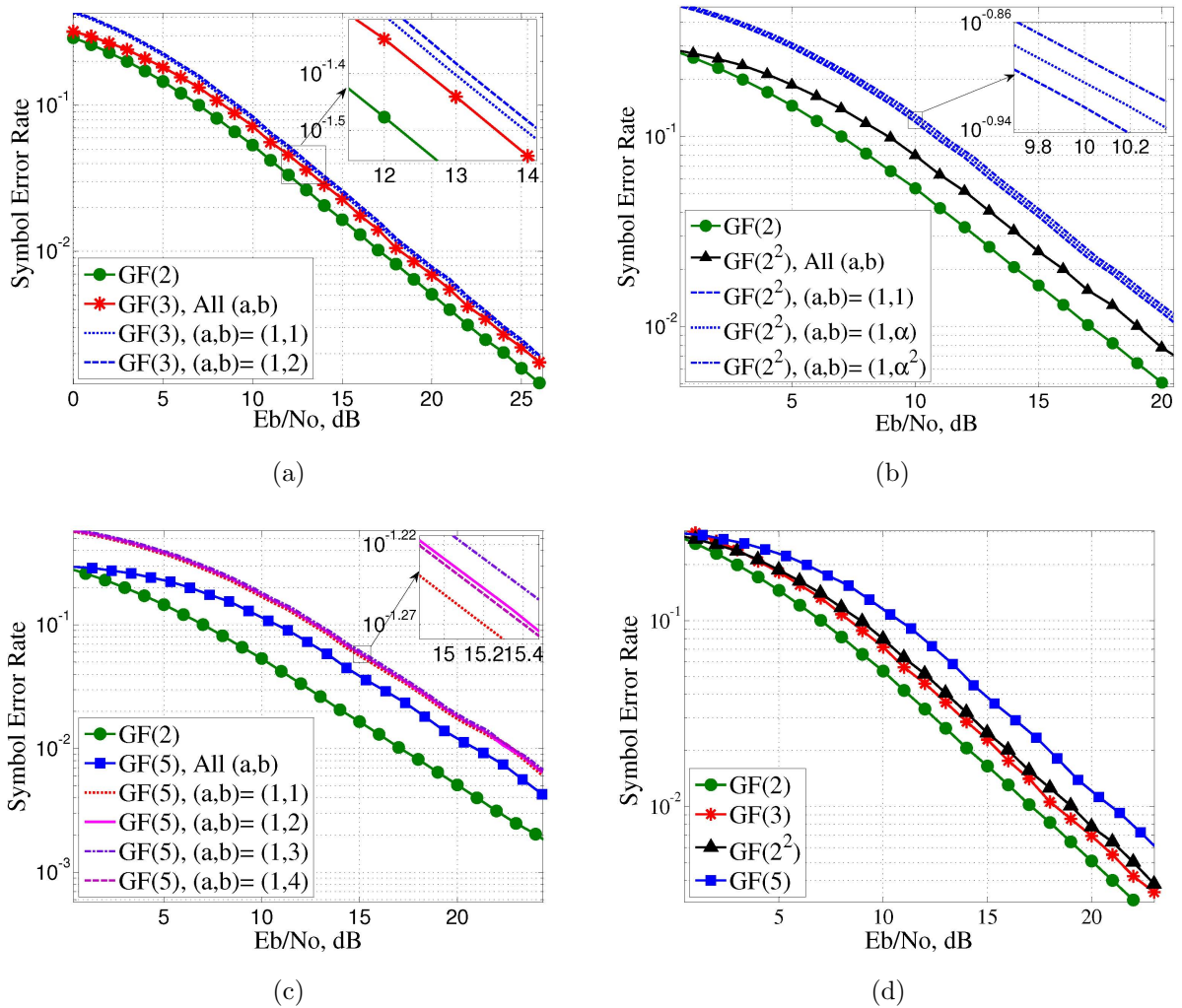

Figure 7.1: Simulation results for un-encoded binary and non-binary: (a) $GF(3)$ and binary, (b) $GF(2^2)$ and binary, (c) $GF(5)$ and binary, (d) comparison of SER performance for $\mathbb{F} = GF(q)$, $(q = 2, 3, 4, 5)$ fields when attempting to decode against all effective combinations

7.2 Concatenated Reed-Solomon/Convolutional Code

For a fair comparison in terms of complexity, the number of states of the convolutional codes should be approximately the same. We choose the number of states to be 2^5, 3^3, 4^2, and 5^2 for $GF(2)$, $GF(3)$, $GF(2^2)$, and $GF(5)$ fields, respectively. The convolutional code rate is 1/2. The best generator polynomial for each field was found by exhaustive search. Table 7.1 shows these generator polynomials.

Comparable Reed-Solomon codes should have the same input and output packet lengths, as well as the same rates. Here, we assume that RS code rate is 0.8. Therefore, the concatenated RS-CC code rate is $0.8 \times 0.5 = 0.4$. Table 7.1 also provides the Reed-Solomon parameters used in this thesis.

Table 7.1: Concatenated RS-CC Parameters for Different Fields

Field	CC gen. poly.	RS (n, k, m)
$GF(2)$	(1 0 1, 0 1 1)	(63, 51, 6)
$GF(3)$	(2 0 1 1, 2 2 2 1)	(59, 47, 4)
$GF(2^2)$	(1 1 1, 1 α 1)	(63, 51, 3)
$GF(5)$	(1 1 3, 2 4 1)	(55, 45, 3)

7.2.1 Quasi-Static Fading Channel Model

Fig. 7.2 illustrates the performance of the binary and non-binary RS-CC encoded in PNC scenarios for quasi-static fading channels. As can be seen from Fig. 7.2(a), attempting to decode against all choices of coefficients (a, b), decreases the frame error rate in a manner equivalent to a gain of approximately 0.6dB in E_b/N_0. Similarly, for other fields, decoding against all choices of coefficients decreases the FER. This decrease in FER for higher order fields, i.e., $GF(2^2)$ and $GF(5)$, as illustrated in Fig. 7.2(b) and (c), is greater since the number of choices of decoding coefficients (a, b) increases as the size of the field increases, according to *Theorem* 1. Thanks to the RS-CC error correcting code, higher order fields outperform the binary case by $1 - 2.5$dB at FER of 10^{-2}, for quasi-static fading channels, with $GF(3)$ providing the best performance. Fig. 7.2(d) shows this fact. For the selected RS-CC coding scheme, the four different constellation mappers shown in Fig. 5.1 have the same FER performance, hence their curves have overlapped in Fig. 7.2(d). Moreover, Fig. 7.2(d) illustrates that the performance of RS-CC encoded curves are approximately $2.5 - 4$dB away from the lower bounds (6.8).
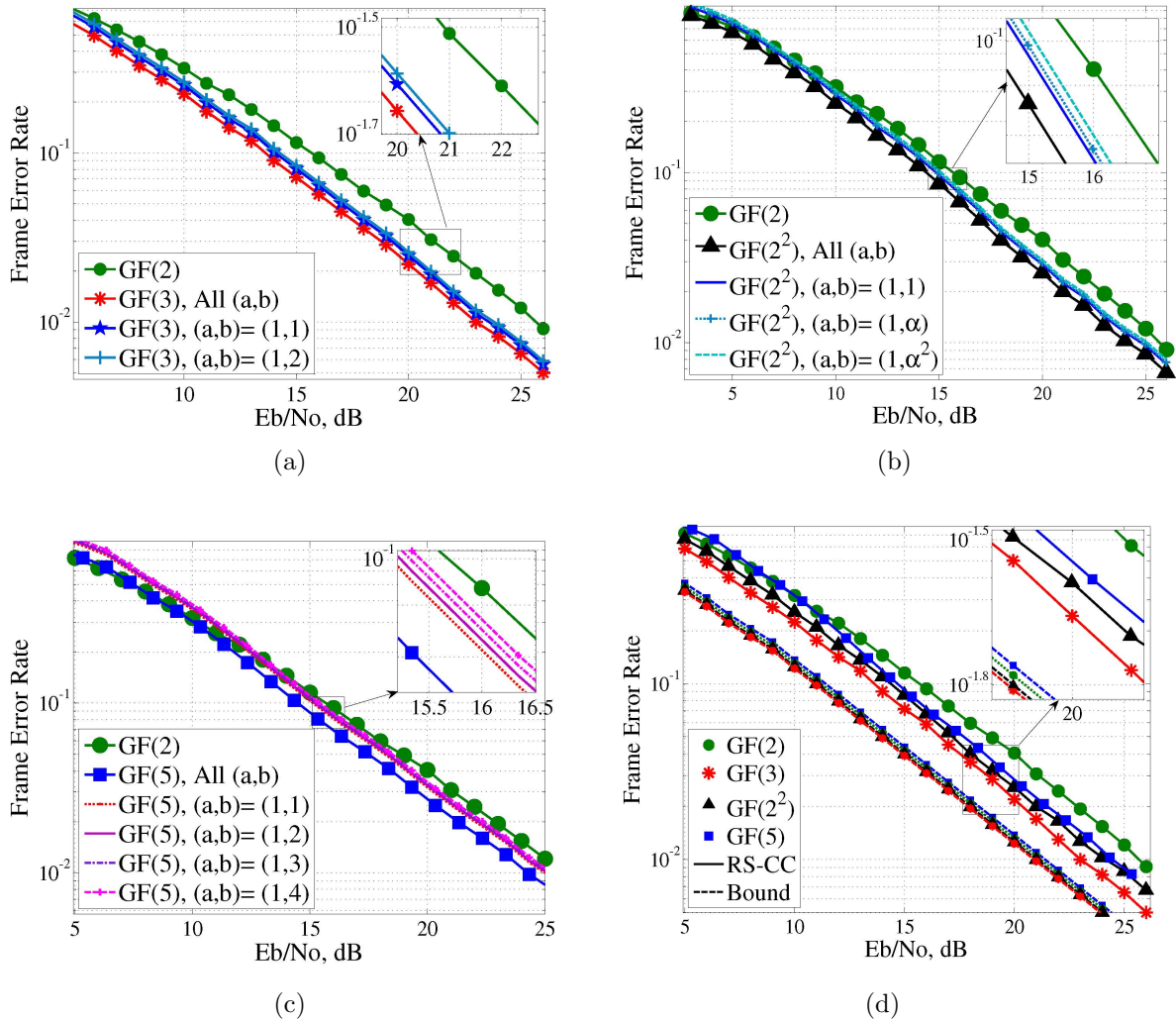
Figure 7.2: Simulation results for binary and non-binary RS-CC encoded for quasi-static fading channels: (a) $GF(3)$ and binary, (b) $GF(2^2)$ and binary, (c) $GF(5)$ and binary, (d) comparison of FER performance for $\mathbb{F} = GF(q)$, $(q = 2, 3, 4, 5)$ fields and the lower bounds (6.8) if the relay attempts to decode against all effective combinations.

Also from Fig. 7.2(d), the $GF(3)$ curve has the minimum distance to its correspondence lower bound. As RS-CC coding results in a significant gap form the lower bounds, we also consider LDPC codes.

7.2.2   Fast Fading Channel Model

Fig. 7.3 illustrates the performance of binary and non-binary RS-CC in PNC scenarios for fast fading channels.
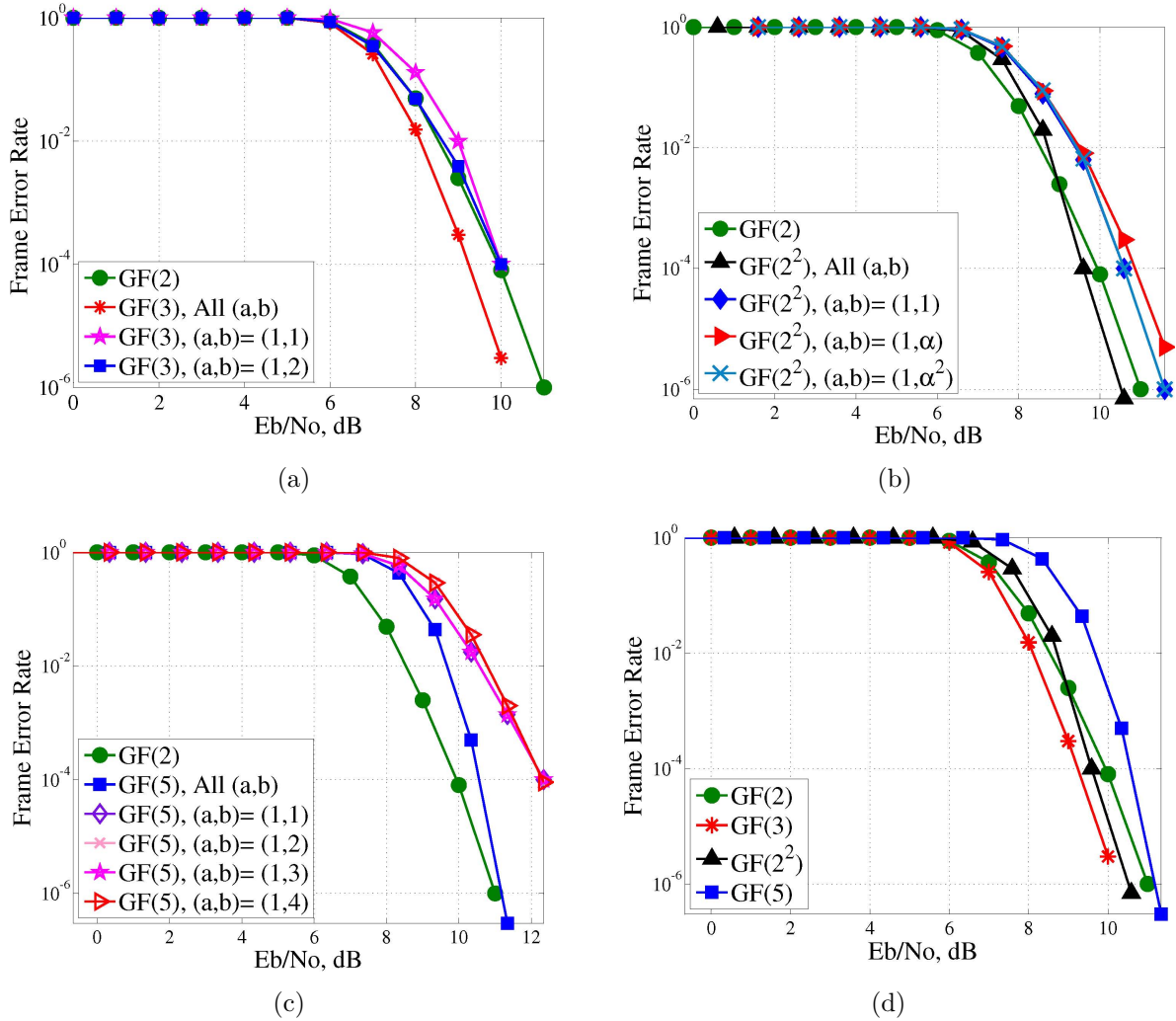

Figure 7.3: Simulation results for binary and non-binary RS-CC encoded for fast fading channel: (a) $GF(3)$ and binary, (b) $GF(2^2)$ and binary, (c) $GF(5)$ and binary, (d) comparison of FER performance for $\mathbb{F} = GF(q)$, $(q = 2, 3, 4, 5)$ fields when decoding against all effective combinations.

As can be seen form Fig. 7.3(a), (b), fields $GF(3)$ and $GF(2^2)$ outperform $GF(2)$

by 0.8dB and 0.5dB at FER of 10^{-4}, but only by taking advantage of decoding against all possible coefficients (a, b). With reference to Fig. 7.3 (a), (b), and (c), attempting to decode against all choices of coefficient (a, b), significantly decreases the frame error rate, providing a gain equivalent to $1 - 2$dB in E_b/N_0 at FER= 10^{-4}.

Finally, Fig. 7.2(d) and Fig. 7.3(d) show that field $GF(3)$ has the best frame error rate performance among all other fields if RS-CC concatenation is adopted at the end nodes.

7.3   Low-Density Parity Check Code

A $(3, 5)$ LDPC code that has a girth-12 graph and a parity check matrix of size 4395×7325 is used for the binary case. The BER performance of this code is 0.8dB away from the Shannon bound at rate 0.4 (-0.22dB). Fig. 7.4 illustrates the BER performance of the LDPC code for the binary field over an AWGN channel. In Fig. 7.4, even at BER of 10^{-7} no error floor is observed, which is an indication of a good parity check matrix design. For higher order fields, some of the ones in the binary matrix are randomly switched to another non-zero element of the field and in this way we construct all the LDPC parity check matrices.
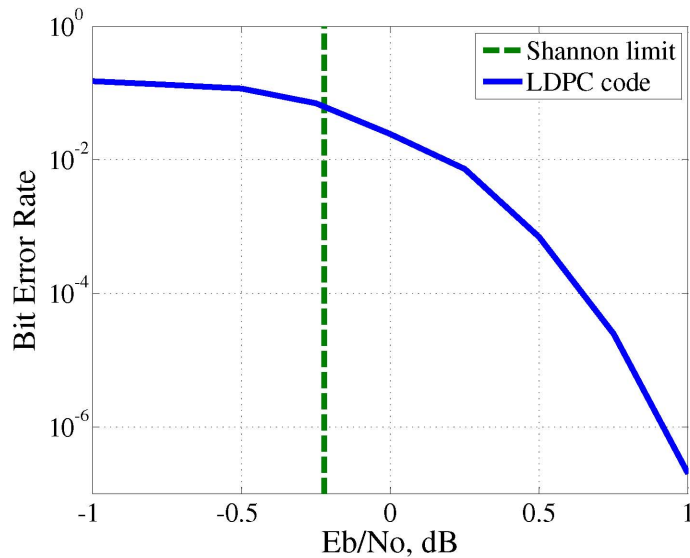

Figure 7.4: Bit error rate of LDPC code and the Shannon limit at the rate 0.4
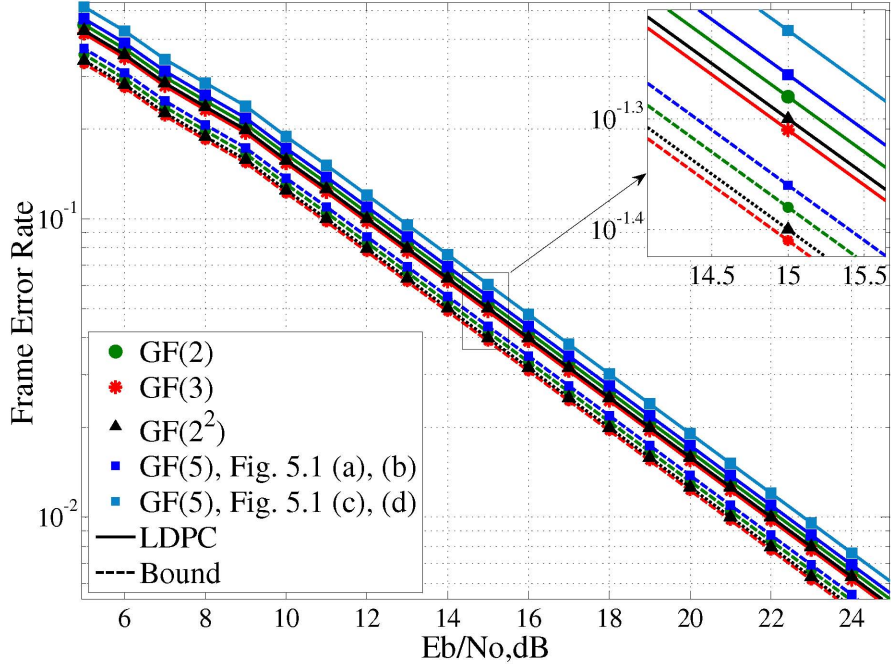
Figure 7.5: Frame error rate for PNC configuration with LDPC coded packets for quasi-static fading channels

7.3.1 Quasi-Static Fading Channel Model

Fig. 7.5 illustrates the performance of the binary and non-binary LDPC codes in PNC scenarios for quasi-static fading channels. For ease of presentation, we do not show the performance by decoding against one set of decoding coefficients in Fig. 7.5 and only the final FER achieved by attempting to decode against all valid coefficients are depicted. Attempting to decode against all choices of coefficients (a, b) decreases the frame error rate by 0.2dB in E_b/N_0. Also, with LDPC coding at the end nodes, the FER performance is found to be only 1dB away from the bound (6.8). For the selected LDPC coding scheme, the constellation mappers shown in Fig. 5.1(a) and (b) have the same performance in terms of FER and they outperform the constellation mappers shown in Fig. 5.1(c) and (d) by about 0.1dB in E_b/N_0. It seems that the constellation mappers Fig. 5.1(c) and (d) themselves have an identical FER performance. Fig. 7.5 also indicates that the non-binary fields, $GF(3)$ and $GF(2^2)$, outperform the binary case by 0.3dB and 0.1dB in E_b/N_0, respectively. However, the binary case has about 0.1dB performance gain compared to the field $GF(5)$. It should also be noted that

fields $GF(3)$ and $GF(2^2)$ can only outperform the binary case by attempting to decode according to all coefficients (a, b), i.e., for a specific pair of decoding coefficients (a, b), binary coding leads to the best performance. Field $GF(5)$, however, performs worse than the binary case even after attempting to decode against all valid coefficients.
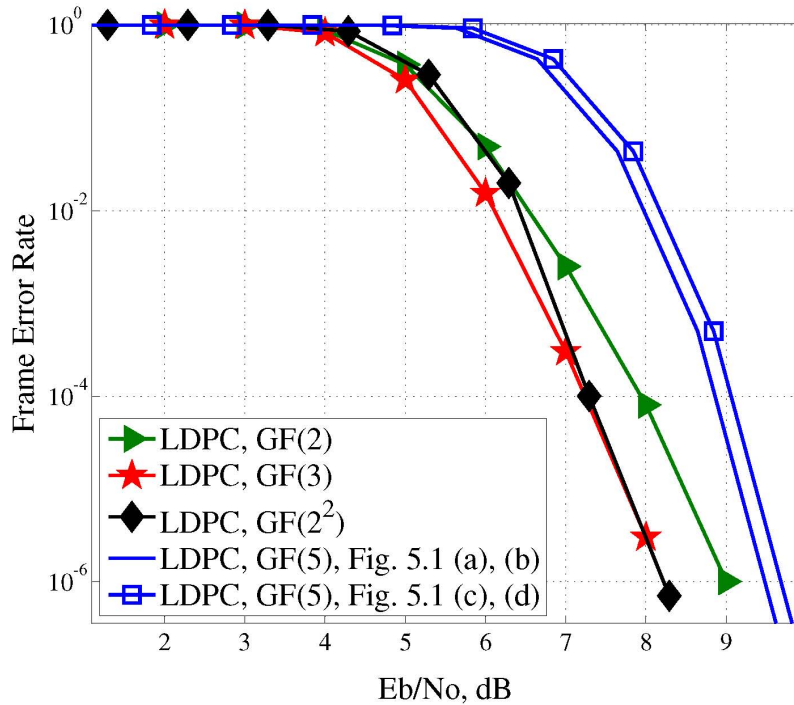

Figure 7.6: Frame error rate for PNC configuration for fast fading channels

7.3.2 Fast Fading Channel Model

Fig. 7.6 illustrates the performance of the binary and non-binary LDPC codes in PNC scenarios for fast fading channels. For ease of presentation, we do not show the performance by decoding against one set of decoding coefficients in Fig. 7.6 and only the final FER achieved by attempting to decode against all valid coefficients are depicted. Using LDPC coding, fields $GF(3)$, $GF(2^2)$ outperform the binary case by 0.7dB at FER of 10^{-4}, but only by taking advantage of attempting to decode against all possible coefficients. However, the binary case outperforms the $GF(5)$ field. Attempting to decode against all choices of coefficients (a, b) also significantly decreases the frame error rate providing a gain equivalent to $1 - 2$dB in E_b/N_0 at FER 10^{-4}.

43

Finally, Fig. 7.5 and Fig. 7.6 show that field $GF(3)$ has the best frame error rate performance among all other fields, employing LDPC coding at the end nodes.

Chapter 8

Conclusion

In this thesis, we have considered a problem of two-way wireless relaying, for which network coding is employed at the physical layer. The end nodes pick their symbols from a field $\mathbb{F}$ and transmit channel-coded PSK-modulated signals to the relay simultaneously. The relay node receives the superimposed channel-coded packets and directly decodes a network-coded combination of the source packets. The channel coding schemes employed are either a practical concatenation of RS-CC codes or LDPC codes. Working over non-binary fields allows the relay to attempt to decode different network-coded combinations, $aS_A + bS_B$ over $\mathbb{F}$, where $a, b \in \mathbb{F}\backslash\{0\}$. We have shown that for a finite field $\mathbb{F}$, there are effectively $|\mathbb{F}| - 1$ unique network-coded combinations. We investigate the performance of different $q-$PSK constellation mappers in terms of FER for $q \leq 5$. We prove that the performance of all mappers in $GF(3)$ is the same in terms of FER. However, in $GF(2^2)$ the performance of different mappers is the same only if a linear code is adopted at the end nodes. For $GF(5)$, if the code is linear, we show that there are 4 different cases of constellation mappers with possibly different performances, which greatly reduces the search space from $5! = 120$ cases to 4. Exploiting the symmetric properties of the problem and using group theory arguments, we have shown that the number of constellation mappers with different performance is much less than the total constellation mappers $|\mathbb{F}|!$. Therefore, we do not need to consider all different constellation mappers. We have found a lower bound using Fano's inequality that confines the FER performance of decoding the network-coded combinations at the relay. Simulation results indicate that finite fields $GF(3)$, $GF(2^2)$, and $GF(5)$ outperform the binary case for quasi-static fading channels if RS-CC channel coding is performed at the end nodes. In addition, for fast fading channels, finite fields $GF(3)$ and $GF(2^2)$ outperform

the field $GF(2)$ only by taking advantage of decoding according to all choices of a and b. Applying LDPC codes for quasi-static fading and fast fading channels, finite fields $GF(3)$, and $GF(2^2)$ outperform the binary case only by taking advantage of attempting to decode multiple network-coded combinations. Finally, simulation results show that the finite field $GF(3)$ has the best probability of error performance among all considered fields.

As future work, it is of interest to consider non-binary constellations for larger systems in which more than two end nodes are communicating.

Bibliography

[1] J. Kim, *Performance Analysis of Physical Layer NetworkCoding.* PhD thesis, The University of Michigan, Ann Arbor, USA, 2009. 1

[2] S.-Y. Li, R. Yeung, and N. Cai, "Linear network coding," *Information Theory, IEEE Transactions on*, vol. 49, pp. 371 –381, feb. 2003. 1

[3] R. Ahlswede, N. Cai, S.-Y. Li, and R. Yeung, "Network information flow," *Information Theory, IEEE Transactions on*, vol. 46, pp. 1204 –1216, jul 2000. 1

[4] R. Koetter and M. M'edard, "An algebraic approach to network coding," *Networking, IEEE/ACM Transactions on*, vol. 11, pp. 782 – 795, oct. 2003. 1

[5] Y. Sagduyu and A. Ephremide, "Joint scheduling and wireless network coding," in *presented at the NetCod 2005*, (Riva del Garda, Italy), Apr 2005. 2

[6] S. Deb, M. Effros, T. Ho, D. R. Karger, R. Koetter, D. S. Lun, M. Mdard, and N. Ratnakar, "Network coding for wireless applications: A brief tutorial," in *In IWWAN*, 2005. 2

[7] Z. Kong, S. A. Aly, E. Soljanin, E. M. Yeh, and A. Klappenecker, "Network coding capacity of random wireless networks under a signal-to-interference-and-noise model," *CoRR*, vol. abs/0708.3070, 2007. 2, 3

[8] S. Katti, H. Rahul, W. Hu, D. Katabi, M. Medard, and J. Crowcroft, "Xors in the air: Practical wireless network coding," *Networking, IEEE/ACM Transactions on*, vol. 16, pp. 497 –510, june 2008. 2, 3

[9] C. Feng, D. Silva, and F. Kschischang, "An algebraic approach to physical-layer network coding," in *Information Theory Proceedings (ISIT), 2010 IEEE International Symposium on*, pp. 1017 –1021, june 2010. 3

[10] S. Zhang, S. C. Liew, and P. P. Lam, "Hot topic: physical-layer network coding," in *Proceedings of the 12th annual international conference on Mobile computing and networking*, MobiCom '06, (New York, NY, USA), pp. 358–365, ACM, 2006. 3, 4

[11] P. Popovski and H. Yomo, "The anti-packets can increase the achievable throughput of a wireless multi-hop network," in *Communications, 2006. ICC '06. IEEE International Conference on*, vol. 9, pp. 3885 –3890, june 2006. 3, 4

[12] B. Nazer and M. Gastpar, "Computing over multiple-access channels with connections to wireless network coding," in *Information Theory, 2006 IEEE International Symposium on*, pp. 1354 –1358, jul 2006. 3

[13] P. Larsson, N. Johansson, and K.-E. Sunell, "Coded bi-directional relaying," in *Vehicular Technology Conference, 2006. VTC 2006-Spring. IEEE 63rd*, vol. 2, pp. 851 –855, may 2006. 4

[14] P. Popovski and H. Yomo, "Bi-directional amplification of throughput in a wireless multi-hop network," in *Vehicular Technology Conference, 2006. VTC 2006-Spring. IEEE 63rd*, vol. 2, pp. 588 –593, may 2006. 4

[15] P. Popovski and H. Yomo, "Physical network coding in two-way wireless relay channels," in *Communications, 2007. ICC '07. IEEE International Conference on*, pp. 707 –712, june 2007. 4

[16] M. Wilson, K. Narayanan, H. Pfister, and A. Sprintson, "Joint physical layer coding and network coding for bidirectional relaying," *Information Theory, IEEE Transactions on*, vol. 56, pp. 5641 –5654, nov. 2010. 5

[17] B. Nazer and M. Gastpar, "Computation over multiple-access channels," *Information Theory, IEEE Transactions on*, vol. 53, pp. 3498 –3516, oct. 2007. 5

[18] B. Nazer and M. Gastpar, "Compute-and-forward: Harnessing interference with structured codes," in *Information Theory, 2008. ISIT 2008. IEEE International Symposium on*, pp. 772 –776, july 2008. 5, 13

[19] S. Zhang, S. C. Liew, and P. P. Lam, "Physical layer network coding," *CoRR*, vol. abs/0704.2475, 2007. 5

[20] S. Katti, S. Gollakota, and D. Katabi, "Embracing wireless interference: analog network coding," in *Proceedings of the 2007 conference on Applications, technologies, architectures, and protocols for computer communications*, SIGCOMM '07, (New York, NY, USA), pp. 397–408, ACM, 2007. 5

[21] S. Zhang, S.-C. Liew, and P. Lam, "On the synchronization of physical-layer network coding," in *Information Theory Workshop, 2006. ITW '06 Chengdu. IEEE*, pp. 404 –408, oct. 2006. 5

[22] M. Valenti, D. Torrieri, and T. Ferrett, "Noncoherent physical-layer network coding using binary cpfsk modulation," in *Military Communications Conference, 2009. MILCOM 2009. IEEE*, pp. 1 –7, oct. 2009. 5

[23] T. Koike-Akino, P. Popovski, and V. Tarokh, "Optimized constellations for two-way wireless relaying with physical network coding," *Selected Areas in Communications, IEEE Journal on*, vol. 27, pp. 773 –787, june 2009. 5, 13, 14

[24] S. Zhang and S.-C. Liew, "Channel coding and decoding in a relay system operated with physical-layer network coding," *Selected Areas in Communications, IEEE Journal on*, vol. 27, pp. 788 –796, june 2009. 6

[25] S. Zhang, S. C. Liew, and L. Lu, "Physical layer network coding schemes over finite and infinite fields," in *Global Telecommunications Conference, 2008. IEEE GLOBECOM 2008. IEEE*, pp. 1 –6, 30 2008-dec. 4 2008. 6

[26] X. S. Zhou, L.-L. Xie, and X. Shen, "Low-density parity-check codes for two-way relay channels," in *Vehicular Technology Conference Fall (VTC 2010-Fall), 2010 IEEE 72nd*, pp. 1 –5, sept. 2010. 6

[27] T. Koike-Akino, P. Popovski, and V. Tarokh, "Denoising strategy for convolutionally-coded bidirectional relaying," in *Communications, 2009. ICC '09. IEEE International Conference on*, pp. 1 –5, june 2009. 6

[28] Y. Wu, P. A. Chou, and S.-Y. Kung, "Information exchange in wireless networks with network coding and physical-layer broadcast," in *Conference on Information Sciences and Systems*, mar 2005. 6

[29] L. Lu, T. Wang, S. C. Liew, and S. Zhang, "Implementation of physical-layer network coding," *CoRR*, vol. abs/1105.3416, 2011. 6

[30] P. Popovski and T. Koike-Akino, "Coded bidirectional relaying in wireless networks," in *New Directions in Wireless Communications Research* (V. Tarokh, ed.), pp. 291–316, Springer US, 2009. 6

[31] B. Nazer and M. Gastpar, "Reliable physical layer network coding," *Proceedings of the IEEE*, vol. 99, pp. 438 –460, march 2011. 6

[32] T. Cover and A. Gamal, "Capacity theorems for the relay channel," *Information Theory, IEEE Transactions on*, vol. 25, pp. 572 – 584, sep 1979. 13

[33] S. J. Kim, N. Devroye, P. Mitran, and V. Tarokh, "Achievable rate regions for bi-directional relaying," *CoRR*, vol. abs/0808.0954, 2008. 13

[34] G. D. Forney, Jr., *Concatenated Codes*. 1966. 23

[35] J. Proakis and M. Salehi, *Digital communications*. McGraw-Hill, 2007. 23, 24

[36] I. S. Reed and G. Solomon, "Polynomial codes over certain finite fields," *Journal of the Society for Industrial and Applied Mathematics*, vol. 8, no. 2, pp. 300–304, 1960. 25

[37] R. G. Gallager, "Low-density parity-check codes," 1963. 25

[38] S.-Y. Chung, J. Forney, G.D., T. Richardson, and R. Urbanke, "On the design of low-density parity-check codes within 0.0045 db of the shannon limit," *Communications Letters, IEEE*, vol. 5, pp. 58 –60, feb 2001. 25

[39] M. Davey and D. MacKay, "Low density parity check codes over gf(q)," in *Information Theory Workshop, 1998*, pp. 70 –71, jun 1998. 25

[40] J. McGowan and R. Williamson, "Loop removal from ldpc codes," in *Information Theory Workshop, 2003. Proceedings. 2003 IEEE*, pp. 230 – 233, march-4 april 2003. 26

[41] P. Hu and H. Zhao, "Improved method for detecting the short cycles of ldpc codes," in *Information Theory and Information Security (ICITIS), 2010 IEEE International Conference on*, pp. 841 –844, dec. 2010. 26

[42] A. M. Gaglione and N. R. L. (U.S.)., *An introduction to group theory*. Naval Research Laboratory, Identification Systems Branch, Radar Division, Washington, DC, 1992. 29